VIDICON UNIFORMITY

James P. Spratt

General Electric Company

Prepared for:

Defense Advanced Research Projects Agency
Air Force Cambridge Research Laboratories

30 September 1974

UNCLASSIFIED

Security Classification

AD/A003 674

DOCUMENT CONTROL DATA - R & D

(Security classification of title, body of abstract and indexing annotation must be entered when the overall report is classified)

1. ORIGINATING ACTIVITY (Corporate author)
General Electric Company
Space Division/Space Sciences Laboratory
P.O. Box 8555, Philadelphia, Pennsylvania 19101

2a. REPORT SECURITY CLASSIFICATION
Unclassified

2b. GROUP

3. REPORT TITLE

VIDICON UNIFORMITY

4. DESCRIPTIVE NOTES (Type of report and inclusive dates)
Scientific. Final. For Period 1 June 1973 to 30 September 1974.

5. AUTHOR(S) (First name, middle initial, last name)
James P. Spratt

6. REPORT DATE
30 ~~June~~ Sept 1974

7a. TOTAL NO. OF PAGES
~~58~~ 59

7b. NO. OF REFS
10

8a. CONTRACT OR GRANT NO.
F19628-73-C-0267

b. PROJECT NO., Task, Work Unit Nos.
2444 n/a n/a

c. DOD ELEMENT
61101E

d. DOD SUPPLEMENT n/a

9a. ORIGINATOR'S REPORT NUMBER(S)
Final Technical Report

9b. OTHER REPORT NO(S) (Any other numbers that may be assigned this report)
ARCRL-TR-74-0410

10. DISTRIBUTION STATEMENT

A - Approved for public release; distribution unlimited.

11. SUPPLEMENTARY NOTES
This research was supported by the Defense Advanced Research Projects Agency. ARPA Order No. 2444.

12. SPONSORING MILITARY ACTIVITY
Air Force Cambridge Research Laboratories
Hanscom AFB, Massachusetts 01731
Contract Monitor: Benjamin R. Capone/LQD

13. ABSTRACT

This program has as its goal the determination of the theoretical and experimental limits of the uniformity of silicon-metal Schottky barrier array vidicon targets. The problem involved in employing high beam velocity operation with silicon diode arrays have proven somewhat more difficult to solve than anticipated. Specifically, the technical problem which has provided the biggest hurdle to successful infrared imaging has been the inability to achieve the anticipated (and required) high diode impedance level under the conditions that exist on a retina subject to high velocity scanning. Consequently work under this program has concentrated on developing a more complete understanding of the characteristics of a beam interrogated Schottky diode. As a result of this effort, a much more realistic model has been developed of high beam velocity vidicon targets than existed previously. This model has led to an improved retina design which avoids previous problem areas, and is being studied under the continuing program (F19628-74-C-0142). It is expected that this new retina design will permit successful imaging with a metal-silicon Schottky barrier array vidicon target.

DD FORM 1 NOV 68 1473 REPLACES DD FORM 1473, 1 JAN 68, WHICH IS OBSOLETE FOR ARMY USE.

1.

UNCLASSIFIED

Security Classification

(59)

14 KEY WORDS	LINK A		LINK B		LINK C	
	ROLE	WT	ROLE	WT	ROLE	WT
Infrared vidicons						
Schottky barrier diode arrays						
High beam velocity vidicons						
Deltacon						

ARPA Order Number
2444

Program Code Number
4010

Name of Contractor
General Electric Company

Effective Date of Contract
1 June 1973

Contract Number
F19628-73-C-0267

Principal Investigator and
Phone Number
J.P. Spratt (215) 962-2555

AFCRL Project Scientist and
Phone Number
B.R. Capone (617) 861-2226

Contract Expiration Date
31 August 1974

Qualified requestors may obtain additional copies from the Defense Documentation Center. All others should apply to the National Technical Information Service.

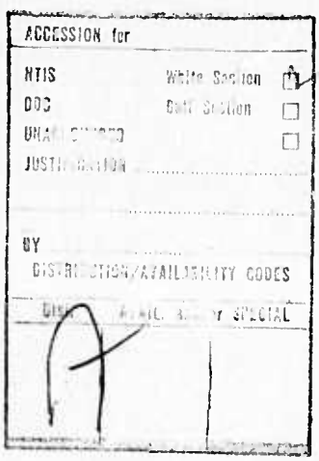

VIDICON UNIFORMITY

I. SUMMARY

A. Technical Problem

The ability to form images using infrared radiation has become increasingly important to the military. In the past ten years, the techniques for performing this task have improved dramatically and appetites have now been whetted to the point where widespread deployment of infrared imagers is being demanded. Unfortunately, the recent progress in imagery has not been matched by reductions in cost. FIRS (Framing Infra-Red Systems) continue to be so expensive as to preclude use in many of the applications desired. The reasons for these high costs are many and complex, and DDR&E is actively exploring ways to reduce them. One factor which has been shown to contribute is the use of exotic detector materials for which no other widespread applications exist. Because of the unique requirements of FIRS, each system requires, in effect, a materials research program to develop the detectors needed. Little advantage has been taken of the tremendous sums spent by the government and private industry over the last ten years in developing silicon integrated circuit technology, since silicon devices do not normally permit the detection of infrared (except for the very near IR). It has recently been realized, however, that silicon technology could be used to advantage in infrared imagers. [1,2]

Internal photoemission in metal-silicon Schottky barrier diode structures has long been known to permit the detection of infrared radiation of wavelengths longer than the fundamental absorption edge in silicon. This process, while generally analogous to photoemission into vacuum, has certain features which are unique and have no direct counterpart in the older technology, e.g. photoemission of holes as well as electrons. The former is interesting because it permits the attainment of low barriers (therefore long cut-off wavelengths) with high work function photocathodes, such as the precious metals (Au, Ag, Pt, Pd). The quantum efficiency of internal photoemission is low, as shown by the modified Fowler relationship. [3]

$$\text{Q.E.} = CA \quad \frac{(h\nu - \phi_o)^2}{h\nu}$$

where Q.E. = quantum efficiency

C = constant $\approx$ 0.1/e.v.

A = optical absorptance

ϕ_o = barrier height

Usint the value for barrier height obtained in the Pd-Si system (ϕ_o = 0.34 e.v.) one obtains a Q.E. $\approx$ 0.1% at a wavelength of 2.7 μm. While this value is low compared to that attainable with photoconductive or photovoltaic detectors, the ability to fabricate these devices in large arrays recommends their use for electron beam scanned infrared vidicon retinae ($\lambda > 1$ μm), where storage mode operation permits one to overcome to some extent the disadvantages of low efficiency.

B. General Methodology

This program has as its goal the determination of the theoretical and experimental limits of the uniformity of silicon-metal Schottky barrier array vidicon targets. (It is being conducted in parallel with Contract No. F19628-73-C-0221, "Infrared Vidicon Development," aimed at showing the feasibility of a camera tube employing such targets.) The specific material system selected for study was palladium silicide on P-type silicon. (Metal silicides on silicon most closely approach ideal metal silicon diodes, since no silicon dioxide insulating layer can form at the interface to interface with carrier transport there.) With this diode polarity it is necessary to interrogate the retina with an electron beam which lands at high velocity ($V_p \approx 200$ volts). Such a beam will generate secondary electrons, and charge the diode array positively. (Conventional P on N silicon diode array vidicon targets operate in the low beam velocity mode, where the beam charges the diode array negatively.) While such operation has been shown by Dresner [4] using Sb_2S_3 targets, it has never been widely used, and no attempts to use it in conjunction with silicon diode arrays have been reported.

The approach taken to this program is as follows:

1. Develop a theoretical understanding of high beam velocity operation of vidicon camera tubes. The structure of such tubes should be extremely important in determining imaging uniformity, e.g. the spacing between target and collecting mesh will affect redistribution of secondaries, temperature of the retina/mesh structure will affect target leakage and mesh spacing, etc.

2. Determine the uniformity of imagery produced under the parallel program.

3. Relate the experimentally determined uniformity to the above mentioned theory, and to structural and material characteristics of the retinas.

C. Technical Results

The problems involved in employing high beam velocity operation with silicon diode arrays have proven somewhat more difficult to solve than anticipated. Specifically, the technical problem which has provided the biggest hurdle to successful infrared imaging has been the inability to achieve the anticipated (and required) high diode impedance level under the conditions that exist on a retina subject to high velocity scanning. Consequently work under this program has concentrated on developing a more complete understanding of the characteristics of a beam interrogated Schottky diode. As a result of this effort, a much more realistic model has been developed of high beam velocity vidicon targets than existed previously. This model has led to an improved retina design which avoids previous problem areas, and is being studied under the continuing program (F19628-74-C-0142). It is expected that this new retina design will permit successful imaging with a metal-silicon Schottky barrier array vidicon target.

D. DoD Implications

While the progress made to date in applying silicon I.C. technology to infrared imagery has not progressed as fast as our original estimates, the eventual success of this effort still appears quite promising. The theoretical and experimental work done under this program have contributed substantially to this goal, since they have enabled Schottky barrier arrays to be designed for operation in an electron beam accessed mode. Experimental efforts aimed at demonstrating imagery and the resultant uniformity can now proceed.

In addition, however, the theoretical results of this program are felt to have implications beyond this program. High beam velocity operation should be applicable to visible camera tubes as well as infrared. Superior performance is expected in uniformity and reduced lag, especially at low light levels. In view of the serious problem encountered in these areas with present low light level TV systems, these performance advantages would be quite useful.

II. DETAILED TECHNICAL DISCUSSION

A. Theory of High Beam Velocity Vidicon Operation

Conventional vidicon camera tubes use photosensitive layers which are continuous, such as Sb_2S_3. Whether such layers are employed in the low beam velocity mode (where the electron beam lands at low energy and charges the retina surface down to ground potential) or in the high beam velocity mode (where the electron beam lands at high energy and charges the retina surface positive with respect to the mesh), the retina is nominally uniform in composition across the sensitive region. Diode array vidicon targets, on the other hand, vary substantially in composition across the surface, having regions of exposed oxide in addition to diode array itself. Also, the silicon surface below the oxide plays a key role itself in target operation. Therefore, to understand the operation of silicon-metal Schottky barrier array vidicon targets, it is necessary to consider the interaction between the electron beam and each of these regions.

1. Potential of metal array

Conventional camera tubes use electron beams which land at a few volts potential to charge individual picture elements to the negative potential at which the cathode of the electron gun sits. Because of the polarity of the diodes used in these retinae, it is necessary to use an electron beam landing at an energy sufficiently high to dislodge secondary electrons with a yield $\delta > 1$, thereby charging individual picture elements positively.[4] Figure 1 shows a schematic of high beam velocity camera tube. The collector mesh is a high transparency screen used to collect secondaries from the target surface (the Pd_2Si array). The combined action of the beam current, I_B, and the secondary emission current going to the mesh, I_M, will charge the floating target surface to a potential V_{FT}.

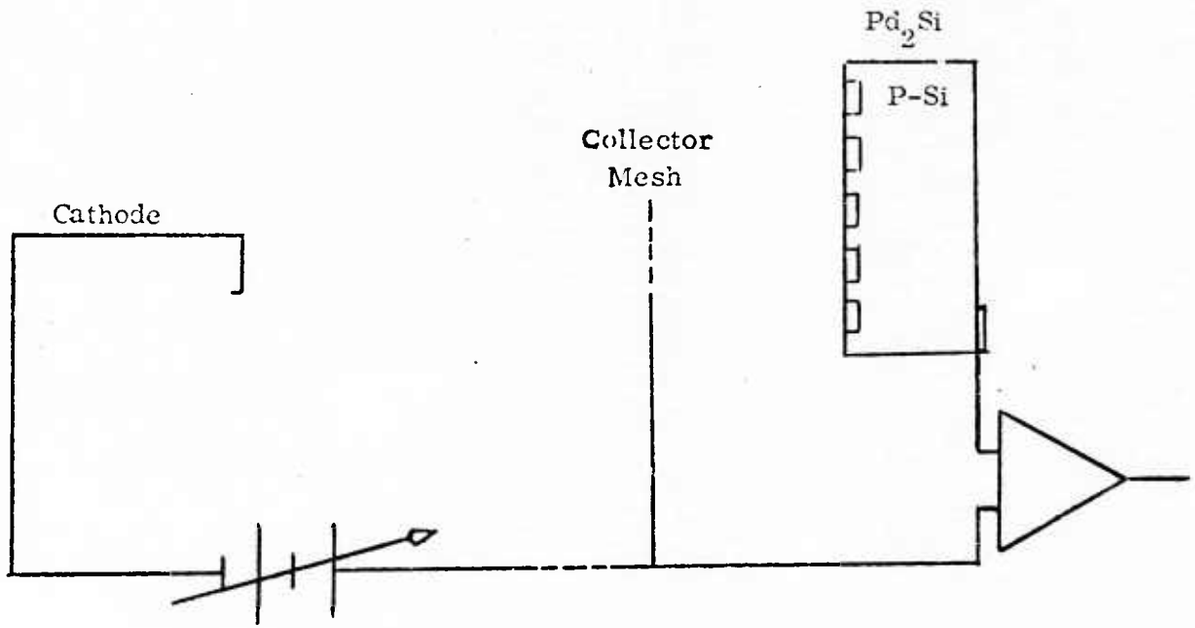

Figure 1. Schematic Diagram of High Beam Velocity Camera Tube

$$V_{FT} = \overline{V}\,\ell n\,\delta$$

where $\overline{V}$ = average energy of secondaries.

If an electron beam is scanned across a retina in raster fashion, and if it is assumed that the exposed oxide between adjacent Schottky diodes plays no role in the process, then the beam will charge the entire diode array to V_{FT}. Optically induced leakage will discharge the target surface down toward mesh potential during the frame time, so that a signal will be generated between retina and mesh when the beam returns during the next scan. The details of this process are presented in Appendix A for the idealized case where no secondaries are generated from the mesh and the oxide surface between adjacent diodes is maintained at silicon potential. In this case, one can describe the operation of a high beam velocity tube by means of the equivalent circuit of Figure 2. Here, the secondary emission between floating target (metal array) and mesh is represented by the current generator $(\delta-1)I_B$ and the resistor r_b, and the Schottky diode is represented by the parallel combination of a photocurrent generator, I_{ph}, a junction capacitor, C_{TS}, and a junction resistor, r_D. The switches in the mesh to target loop are closed during the read time, t_R, and are open during the storage time, $t_F - t_R$ (t_F = frame time). This equivalent circuit, and the mathematical analysis associated with it, are very useful in analyzing the performance obtained in actual vidicons of this type, despite the high degree of idealization involved. For example, under conditions of uniform, time independent illumination, it can be shown that a d.c. signal current is generated which is related to tube and retina parameters as follows: (Cf. Appendix A for clarification)

$$I_s = n\left[\frac{r_b}{(r_b+r_D)}(\delta-1)I_B + \frac{r_D}{(r_b+r_D)}\left\{y\,i_{ph} + \frac{V}{r_D}\right\}\right]$$

$$\left[1 + \frac{r_D}{r_b}\,\frac{C_{r_{11}}}{t_f}\,f\right]$$

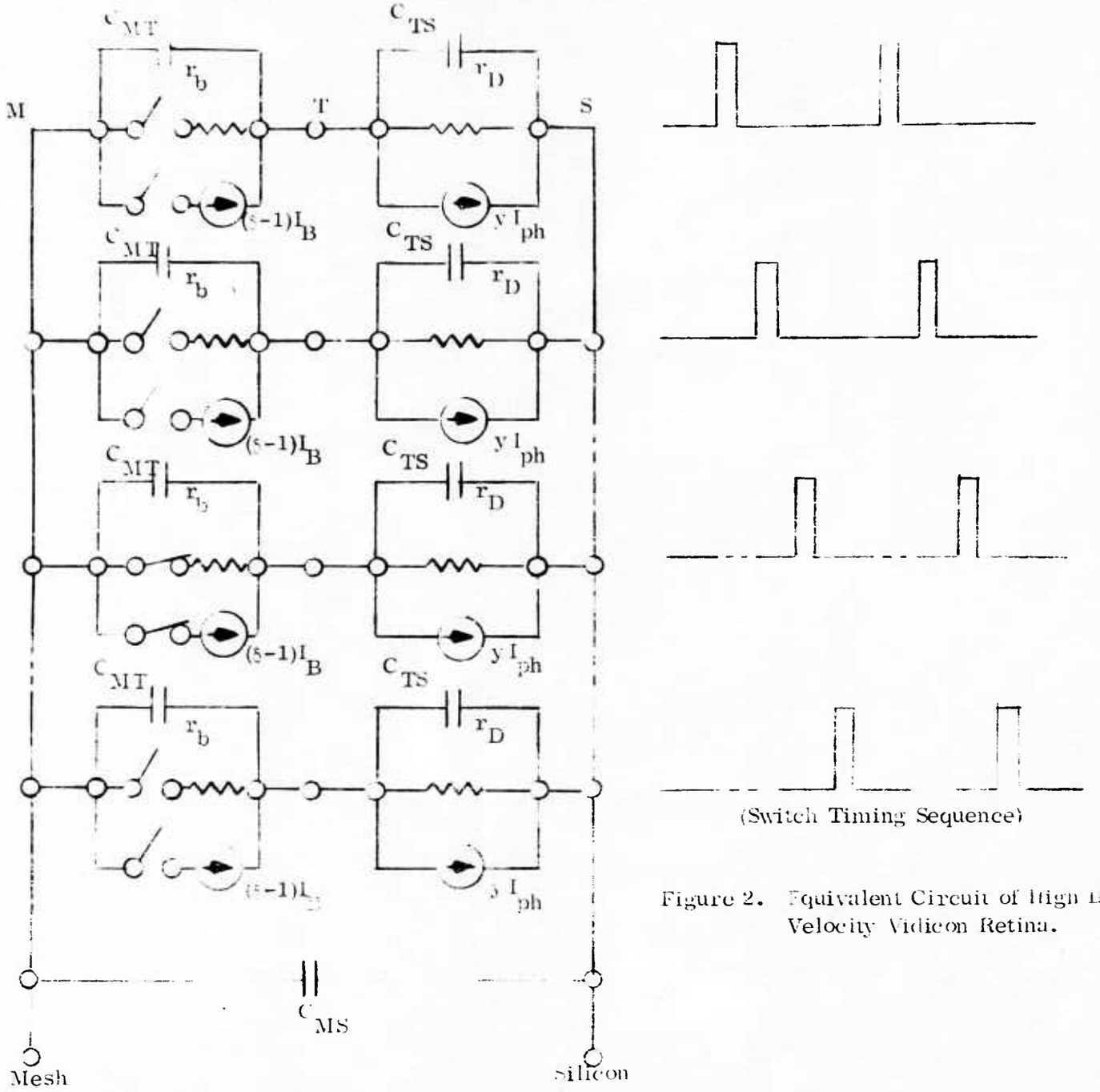

Figure 2. Equivalent Circuit of High Beam Velocity Vidicon Retina.

where n = number of diodes under the beam at any given time

I_B = beam current

y = diode responsivity in amps/watt

i_{ph} = light power in watts

V = target bias

r_{11} = parallel combination of r_b and r_D

f = fraction of maximum voltage excursion which diodes actually experience

This equation suggests a number of diagnostic measurements which may be made under uniform illumination conditions, e.g.

$$\frac{dI_S}{dI_B} = n(\delta - 1) \frac{r_b}{r_b + r_D} A; \qquad \frac{dI_S}{dV} = n \frac{1}{r_b + r_D} A$$

$$\frac{dI_S}{d(yi_{ph})} = n \frac{r_D}{r_b + r_D} A$$

where A = tube amplification factor

$$\left[= 1 + \frac{r_D}{r_b} \frac{C r_{11}}{t_R} f \right]$$

By measuring these quantities vs. temperature (thereby varying r_D/r_b) the elements of the equivalent circuit can be obtained.

Experimental work on high beam velocity vidicons, using a demountable camera tube designed and built under a parallel program [5], has shown that the retina impedance (r_D) was not sufficiently high to achieve storage mode gain (Cf. Section II, B). In the course of investigating the reasons for this problem, the assumption that the oxide surface was maintained at the potential of the silicon was re-examined. It was found that this assumption was not fulfilled in the retina design used to date. The following discussion considers the potential of the surface of an SiO_2 layer under an electron beam.

2. Potential of the SiO_2 surface being scanned by an electron beam

To determine the potential of the surface of the SiO_2 between adjacent metal islands in the array, consider the situation which exists when the retina is scanned by the beam while at room temperature. Because of the low barrier heights required in the metal-silicon Schottky barriers for the desired infrared cutoff, the diode impedance at room temperature is low, and the metal island can, in this case, be regarded as sitting at silicon potential relative to the cathode (V_{TK}). If this potential is increased from zero, while maintaining the mesh at a slight positive potential (V_{MT}) relative to the silicon, it is desired to calculate the potential at which the SiO_2 surface will float in the geometry used in these retinae. It can be shown that the oxide surface, if it were completely isolated electrically from the target, can sit in two stable states; viz, at a potential slightly negative with respect to the cathode potential where the beam has been cut off, or at a potential slightly positive relative to the mesh where secondaries are being emitted to the mesh at a rate just equal to the beam current. In actual practice, the oxide surface is in contact with the target, where the target metal joins the oxide.

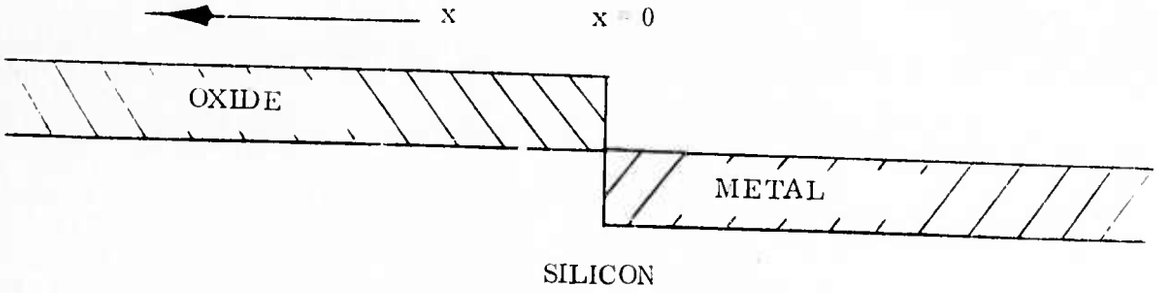

Figure 3

Therefore the potential of the oxide surface immediately adjacent to the metal must sit at the metal target potential, and the beam must supply a net flow of electrons in or out of the oxide in this region depending on whether $j_b \left[\delta (V_T) - 1 \right]$ is less than or greater than zero. Here $\delta (V_T)$ is the secondary emission ratio of the oxide if the oxide surface sits at target potential. If the electrons are generated in the oxide with sufficient energy to escape as secondaries, it would seem that while the beam is landing, there should be electrons in the conduction band of the oxide, at least in a thin skin near the surface. These electrons can conduct laterally along the surface. Therefore,

the oxide would have a sheet conductance σ under the influence of the beam. The lateral current/unit width in the oxide surface would then be given by

$$j = -\sigma \frac{dV}{dx} \text{ , where } \sigma \text{ is in mhos} \tag{1}$$

if lateral voltage gradients occur. The derivative of the lateral current would be given by

$$\frac{dj}{dx} = j_b \left[1 - \delta(V) \right] \tag{2}$$

In actual practice, σ is no doubt a function of V, the landing voltage.

However for this discussion, we will assume it is constant. Further let us assume that $\delta(V) = V/Vc$,

where Vc is the voltage for which δ goes to unity. Then (1) and (2) may be combined to give

$$\sigma V_c \frac{d^2 (V/V_c)}{dx^2} = j_b \left[1 - \frac{V}{V_c} \right] \tag{3}$$

If the oxide is assumed to be semi-infinite in extent, then as we increase the target voltage above cathode

$$V = V_{TK} \text{ at } x = 0$$

and (4)

$$\frac{dV}{dx} = 0 \text{ at } V \approx 0 \quad (x = W)$$

where the voltages are measured relative to cathode. The solution to (3) which satisfies the boundary conditions (4) is

$$\frac{V - V_c}{V_c} = \left(\frac{V_T - V_c}{V_c} \right) \left[\frac{\sin Ax \sin AW + \cos Ax \cos AW}{\cos AW} \right] \tag{5}$$

where $A = \sqrt{\frac{j_b}{\sigma V_c}}$; $\cos AW = \left[1 - \frac{V_T}{V_c} \right]$

If one combines (5) and (1) to calculate the current flowing into the target by x = 0, we find that the current/unit width of oxide-metal interface is given by

$$j = \sqrt{j_b \sigma V_c} \left(\sqrt{\frac{2V_T}{V_c} - \frac{V_T^2}{V_c^2}} \right) \tag{6}$$

This current has a real solution for

$$0 \leq \frac{V_T}{V_c} \leq 2$$

For V_T/V_c between (1) and (2), there is a net flow of electrons away from the oxide surface near the target but these can be supplied by the larger number of electrons flowing into the oxide surface in the regions where it sits near cathode potential. Therefore the integrated current flowing from the oxide to the target is positive until the target reaches voltages significantly above V_c.

If the target voltage is increased above 2 V_c, there can only be a net flow of electrons from the target to the oxide. The target would no longer be able to charge down to cathode potential, but would have to charge to potentials more positive than the target in order to carry a net electron current away from the metal-oxide interface. As we move away from this interface, the oxide surface continues to go more positive until it reaches approximately the mesh potential. (This assumes that the mesh is more positive than the target.) Once V_T exceeds 2 V_c, the boundary conditions described in (4) must then be changed to

$$\left.\begin{aligned} V &= V_T \quad \text{at } x = 0 \\ \text{and} \\ \frac{dV}{dx} &= 0 \quad \text{at } V = V_M \end{aligned}\right\} \tag{7}$$

The solution to (3) and (7) is again the same as (5) except that now

$$\cos AW = \frac{V_T - V_c}{V_M - V_c} = \frac{V_T - V_c}{V_T + (V_M - V_T) - V_c} \tag{8}$$

When (8) is substituted into (5) the current may be calculated at the target-oxide interface as

$$j = -\sqrt{j_b \sigma V_c}\quad\sqrt{\frac{(V_M-V_T)^2 + 2(V_T-V_c)(V_M-V_T)}{V_c}} \tag{9}$$

As V_T is now reduced back toward cathode potential, j may continue to be negative until

$$V_T - V_c = \frac{-(V_M-V_T)}{2}$$

or until $V_T = V_c - \frac{(V_M-V_T)}{2}$ (10)

Equations (9) and (6) are plotted in Figure 4 for $\frac{V_M-V_T}{V_c} \approx 1$. The arrows indicate the current flow as a function of the direction in which V_T is changed. If W as defined in equations (5) and (8) is greater than half the oxide width between 2 adjacent metal islands, the above equations would have to be modified to correct for the finite width of the oxide.

The foregoing analysis considered the case where the metal islands were at target (silicon) potential. In actual operation, the diode impedance should be sufficiently high that the metal islands will float, just as the oxide surface does. These two regions will float at an average potential set by the individual secondary emission properties. In view of the coupling between these two regions provided by the secondary emission process itself, and by beam induced conductivity in the oxide, it is clear that the entire retina surface will, under high beam landing velocity conditions, float slightly positive relative to the mesh.

3. Surface potential of the silicon

The previous analysis has shown the importance of achieving high diode impedance to the successful operation of metal-silicon Schottky barrier array vidicon targets. This high impedance must be obtained, not in the highly idealized one dimensional diode normally treated in the literature, but in a device having a very large perimeter to area ratio. This geometry is felt to be sufficiently different from normal

Figure 4

Normalized target current per unit length of diode perimeter vs. normalized target voltage

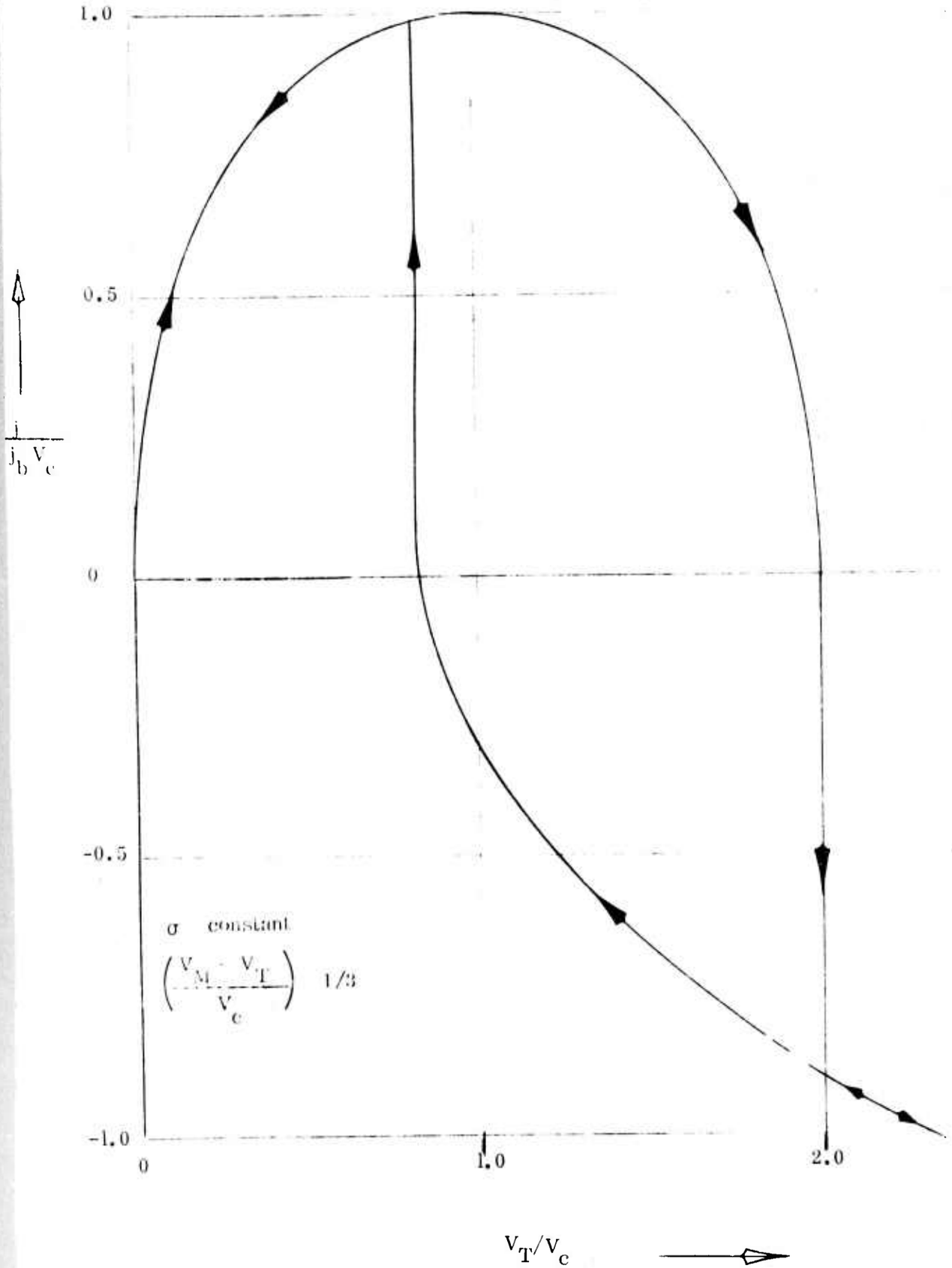

devices to warrant special treatment. Also, the behavior of a Schottky diode being contacted by an electron beam is expected to be substantially different from one contacted by conventional metal electrodes. These two cases will be treated separately.

a. Metal contacts to a Schottky diode array

Figure 5A is a schematic of a metal-silicon Schottky barrier array vidicon target as it might be used in a camera tube. The electron beam scans the diode array side. To characterize these retinae before putting them in a camera tube, it is desirable to perform electrical measurements with a metal layer (later removed) connecting a number of elemental diodes into one large "diode". Figure 5B is a schematic of such a device with a metal overlay. In the latter case, the metal over the SiO_2 cannot supply electrons to the oxide conduction band because of the high barrier at this interface. Consequently, this contact is insulating. To determine the effect of the large perimeter to area ratio of such a device on its current-voltage characteristic, it is necessary to examine the electron energy diagram at the perimeter of a metal island. Figure 6 shows such a diagram where the metal contacts the silicon directly (M-S contact), and where the oxide layer sits between the metal and the silicon (M-O-S contact). Figure 6A shows these two diagrams for zero applied bias. The M-S contact is characterized by a barrier height ϕ_o. In the M-O-S contact, the energy difference between the metal Fermi level (F.L.) and the valence band edge is given by the silicon surface potential, ϕ_s. ϕ_s is determined by the charge concentration in the oxide, works function difference, etc., and may be less than ϕ_o. Electrons at the Fermi level in the metal on plane AA' in Figure 5B will see a barrier height ϕ_o in the x-direction, and ϕ_s in the y-direction. As the metal bias is varied relative to the silicon, ϕ_s varies while ϕ_o is constant. This occurs since the metal F.L. is the same in both the M-S and M-O-S contact, the semiconductor Fermi level is the same in both cases, and some of the potential difference appears across the oxide in the M-O-S case while all of it drops across the depletion layer in the M-S case. Thus, if ϕ_s (V=O) $< \phi_o$, current flow at the periphery will dominate the diode.

Figure 5

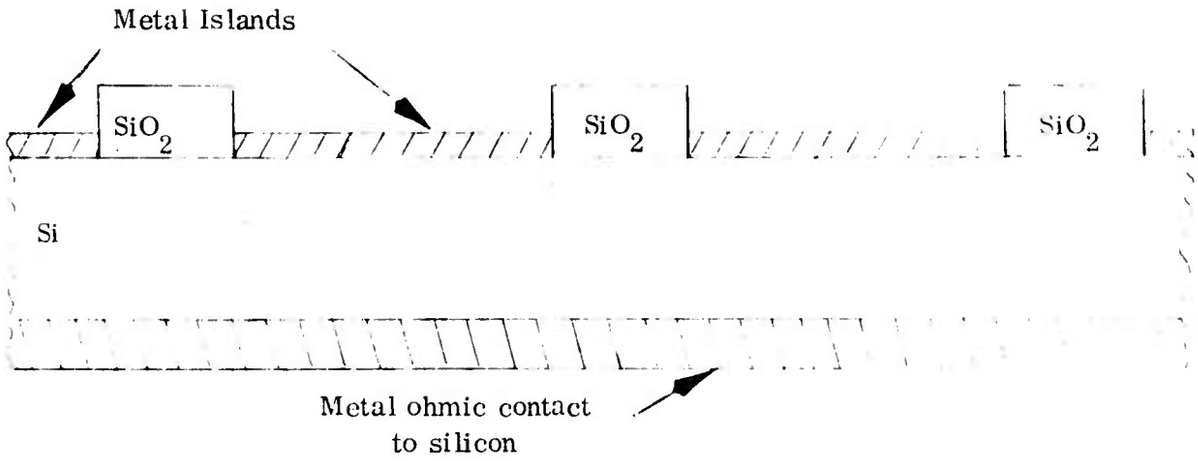

A. Schematic of Schottky barrier array retina

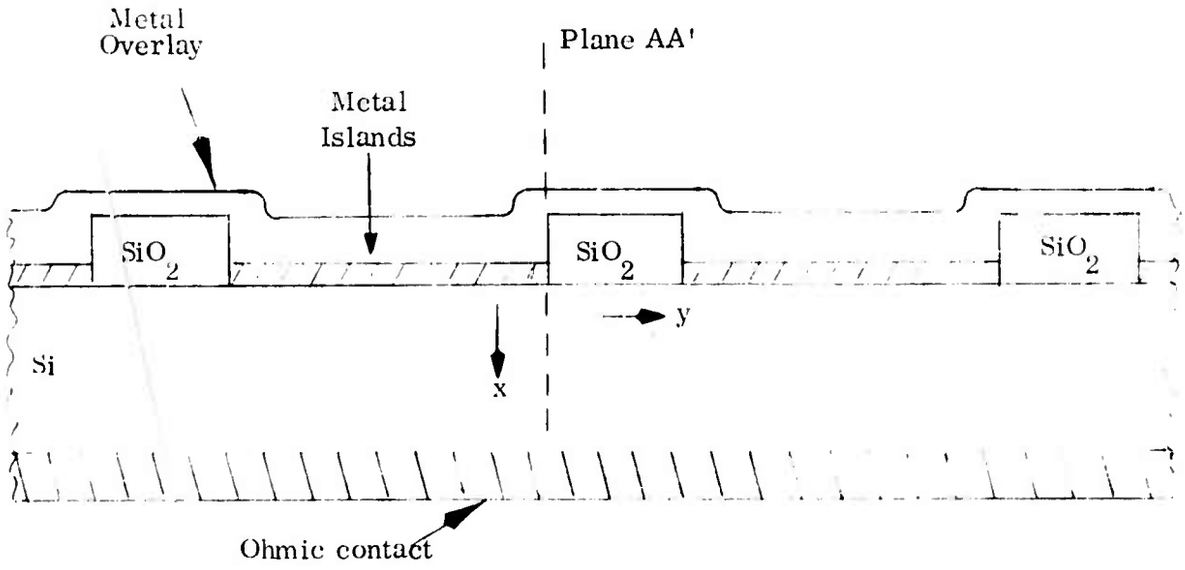

B. Schematic of Schottky retina with metal overlay

Figure 6

Electron potential diagram of Metal - P silicon
Schottky diode, and Metal-oxide - P silicon interface

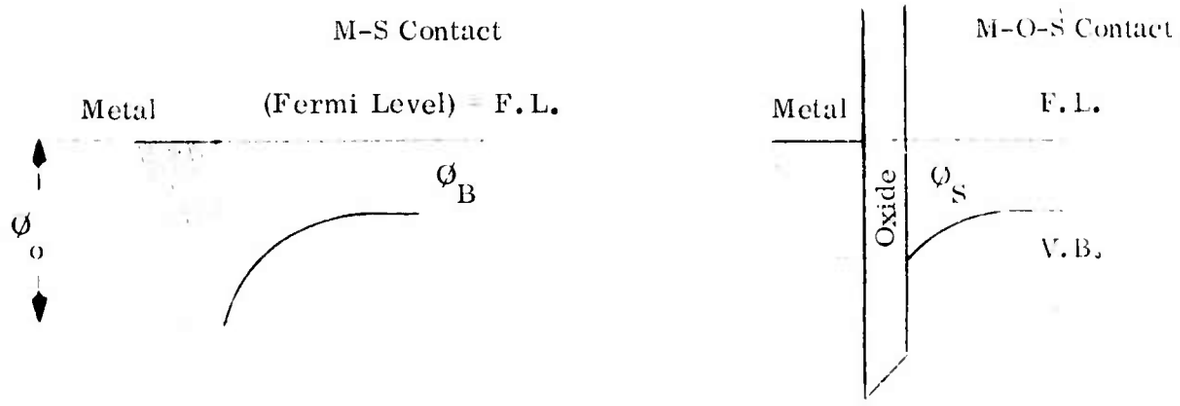

Figure 6A. Zero Applied Voltage

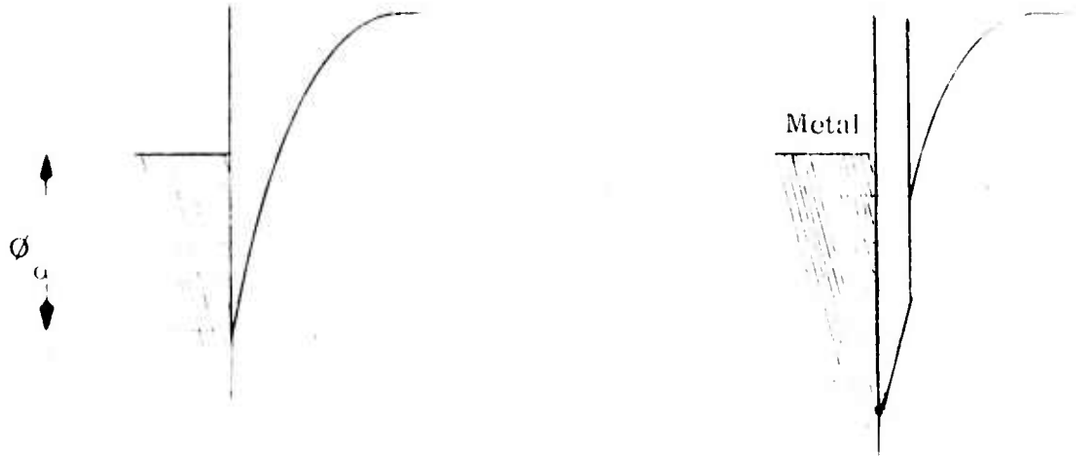

Figure 6B. Reverse Bias Case

Figure 6B. Forward Bias Case

b. Electron beam contact to a Schottky diode array

If an electron beam is used to contact the Schottky diode array shown in Figure 5A, it makes a good "ohmic" contact to the SiO_2, since any electron landing on the oxide automatically finds itself in the oxide conduction band.

Electrons landing at high velocity on the SiO_2 will eject secondaries from the surface, creating (for $\delta > 1$) a net positive charge at the oxide surface. The positive charge is known to be immobile, but the electrons have a relatively high mobility (34 cm^2/V-sec) [6] and will travel through the oxide unless prevented by an opposing field. The mechanism by which this current will be limited is space charge buildup, so that the voltage which must be developed across the oxide to make the oxide high impedance to the landing beam can be calculated from the Mott-Gurney law [7] to be

$$V_{ox} = \left[\frac{8L^3 j_B}{9K\epsilon_o \mu_n}\right]^{1/2}$$

where L = thickness of the SiO_2

j_B = beam current density

μ_n = electron mobility

For typical values (viz $L = 0.5\ \mu m$, $j_B = 10^{-3}$ amps/cm^2, $\mu m = 34$ cm^2/V-sec), the voltage drop across the oxide required to prevent the landing beam from going through is oxide is only 3 millivolts. It is highly probable that potential differences of this magnitude exist in the oxide inequilibrium. If they do not, they will develop rapidly under the electron beam as beam electrons collect in inversion layers at the silicon - SiO_2 interface. Thus, even though the electron beam makes a good "ohmic" contact to the oxide, space charge buildup makes this layer opaque to the beam.

c. Surface inversion in the silicon under the oxide

Silicon P-N junction vidicon retinae are adversely affected by the existence of inversion layers in the silicon under the oxide. Such layers are a prime cause of "blooming", so that it is natural to ask if similar effects can be expected in Schottky barrier array vidicon retinae. A detailed analysis of this question has shown that

under the expected conditions of operation, surface inversion will not adversely affect retina operation, since there is no way to supply minority carriers to the surface of the silicon. Thermal generation is suppressed by the low retina operating temperature. Optical generation is prevented by filtering out band edge radiation. Finally, since the potential barrier to majority carriers is by definition low (ϕ_h = 0.35 e.v. for Pd_2Si on P-Si), the barrier to minority carriers is high (ϕ_e ($\phi_e = E_g - \phi_h$ = 0.75 e.v.). Therefore, electrons cannot be injected into the silicon from the metal. In the previous section, the possibility of supplying electrons to be surface inversion layer by transport of beam electrons through the SiO_2 layer was discussed. It was shown that, under some conditions, electrons can be supplied to the silicon surface by this process, and these electrons could contribute to the formation of a surface inversion layer. It can be shown, however, that even if such a layer is present, the electrons therein are trapped and cannot discharge the metal contact. This is verified by the potential diagrams shown in Figure 7, which illustrate the surface potential situation under conditions of surface inversion under the oxide. Figure 7A treats the case of zero applied bias across an M-S contact and an adjacent M-O-S contact where the potential of the oxide surface and the metal is common. Figure 7B treats the reverse bias case. It can be seen that electrons in the inversion layer sit approximately at the electron Fermi level, whereas the conduction band edge under the metal sits at ϕ_e above the Fermi level. Thus, they are trapped. Even if adjacent diodes were at different potentials due to optical discharge, these electrons cannot surmount the barrier trapping them under the oxide. This situation is contrasted to that existing in P-N junction retinae, which is shown in Figure 8. Here, electrons trapped under the oxide in an inversion layer see no barrier preventing them from flowing along the surface to an adjacent N region, thereby interconnecting diodes and producing the phenomena of blooming.

3. Summary

The above theoretical discussion has shown that metal-silicon Schottky barrier diode arrays can be operated as infrared vidicon retinae in the high beam velocity mode. The floating target surface (metal islands and exposed SiO_2) will be charged positively relative to the mesh electrode (Cf. Appendix B for a discussion of the alternate

Figure 7

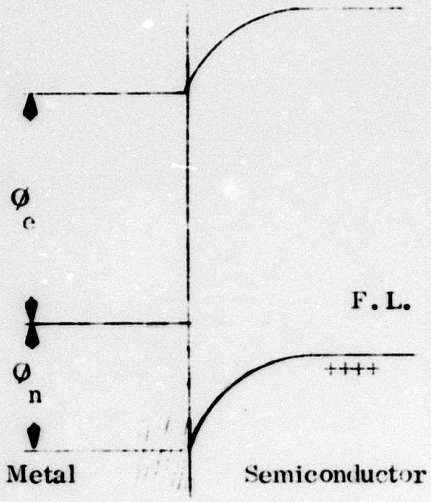

Figure 7A. Electron potential diagrams for metal-semiconductor diode and an adjacent inversion layer at zero bias.

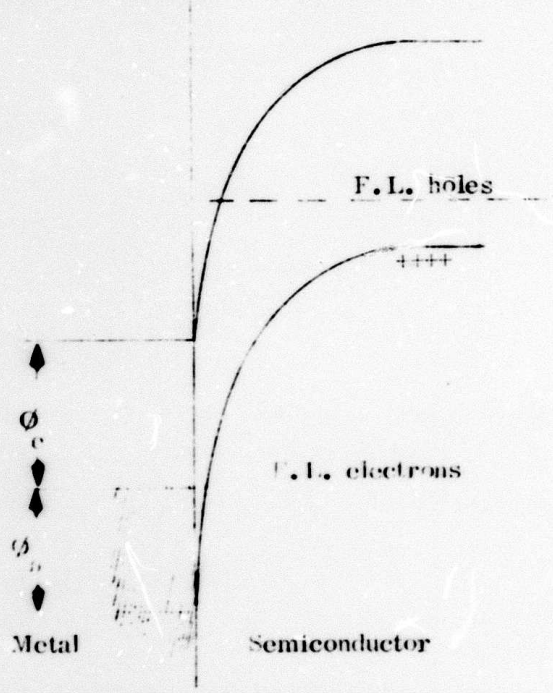

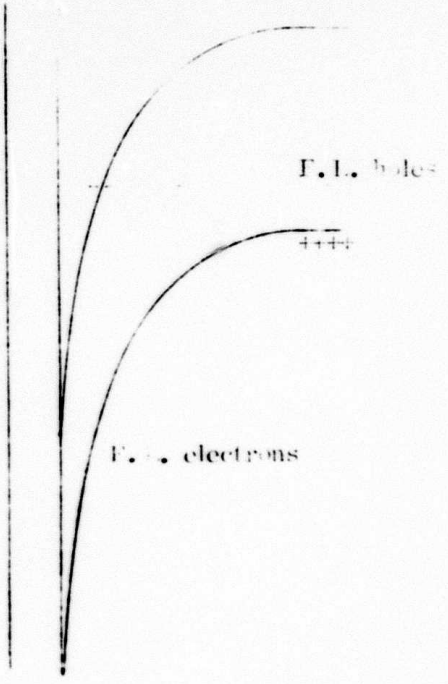

Figure 7B. Electron potential diagram for metal semiconductor contact under bias and an adjacent inversion layer.

Figure 8

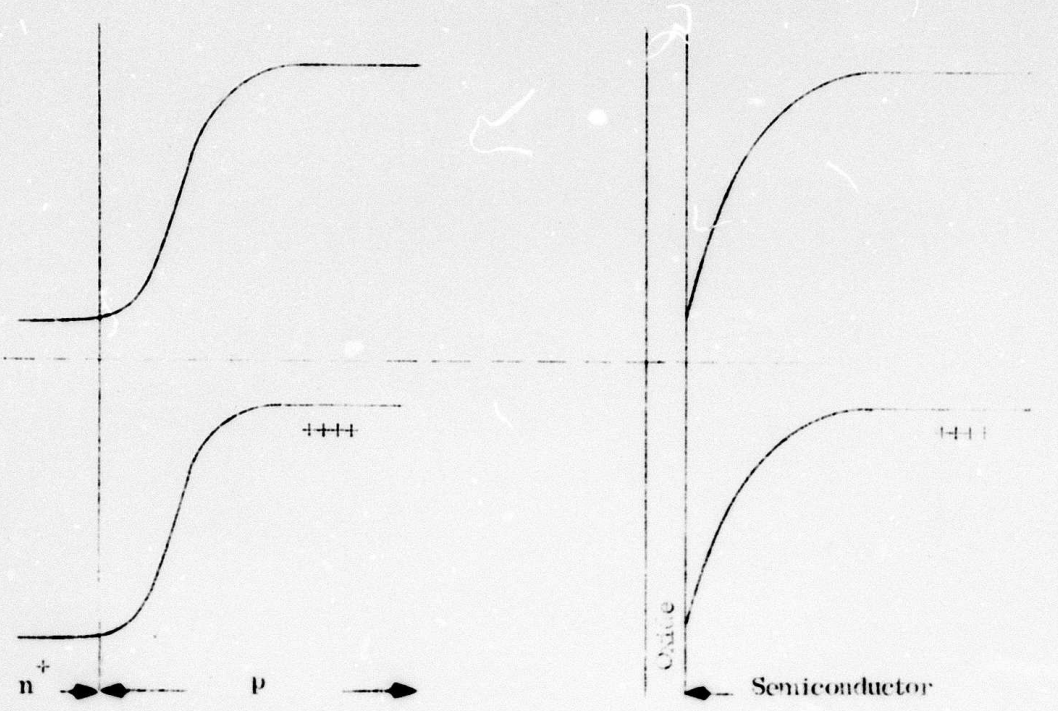

Figure 8A. Electron potential diagrams for p-n junction and an adjacent inversion layer at zero bias.

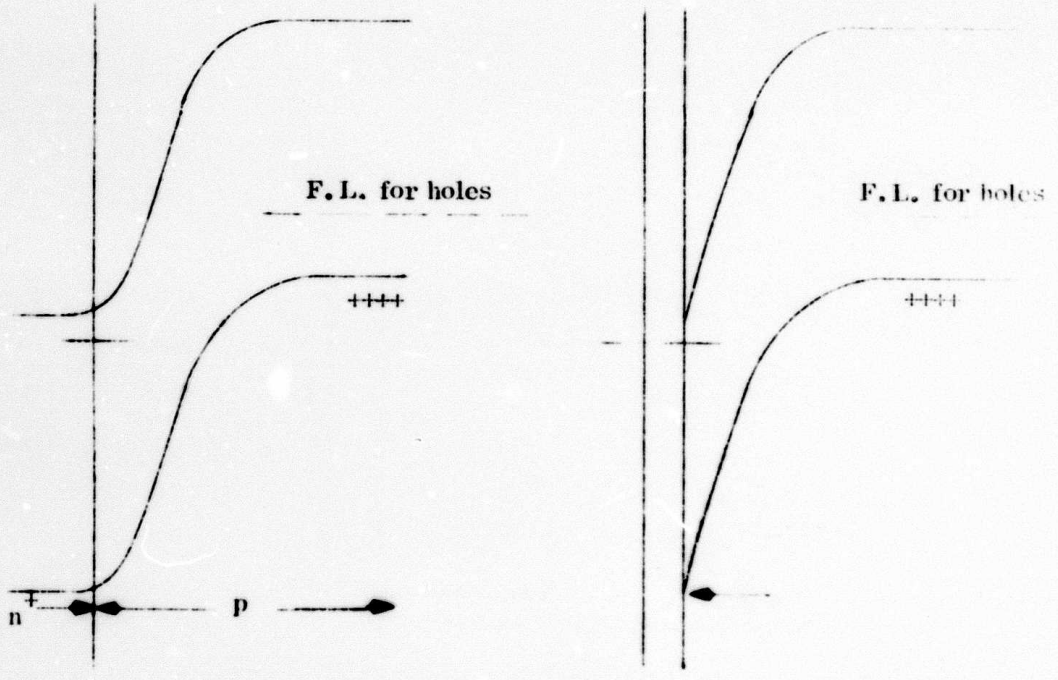

Figure 8B. Electron potential diagram for p-n junction under bias and an adjacent inversion layer.

$$\langle I_s \rangle_{dark} = N \langle i_o \rangle$$

where N is the total number of diodes and $\langle i_o \rangle$ is the average reverse leakage current of the diodes in amperes. In order for this reverse leakage to be unimportant, we would like

$$N \langle i_o \rangle \lesssim 2 \times 10^{-9} \text{ amps} \tag{12}$$

Let
$$i_o \approx 120\, T^2 A \times e^{\frac{-q\phi_o}{kT}} \tag{13}$$

where A is the device area, T is the absolute temperature, q is the electronic charge, k is Boltzman's constant and ϕ_o is the effective barrier to hole flow. Then from (12) and (13)

$$120\, T^2 A\, e^{-q\phi_o/kT} \lesssim 2 \times 10^{-9} \text{ amps} \tag{14}$$

Assuming an active area of target of about 5 cm^2, equation (4) would be satisfied if

$$\phi_o \gtrsim 0.24 \text{ ev at } 77^\circ K$$

and
$$\phi_o \gtrsim 0.31 \text{ ev at } 100^\circ K \tag{15}$$

If the effective barrier height seen by the holes in the Pd is 0.35 ev as determined by the photoelectric threshold, the average daily current would be significantly less than the noise current of the preamps for temperatures below $100^\circ K$.

2. Fluctuations in the Dark Current

The previous calculation would indicate that well-behaved Schottkys should have a very safe margin on the magnitude of the reverse current in the dark, and that for the vast majority of the diodes one might anticipate that the dark current and its fluctuations would be unimportant.

Section II.A above has treated the possibility of excess leakage existing in the retina as a result of barrier lowering at the perimeter of individual Schottky diodes in the retina. Whether this effect is a problem will be determined by the state of charge in the oxide, and good technology could eliminate it. In any case, the use of an integrated mesh would suppress any such effect, so that we will assume then that the

vast majority of diodes can be brought to a state where their dark current is negligible. There will almost surely be some defects in the Si or its surface, however, which could cause occasional diodes to have a very low impedance. These diodes will effectively act as shorts, and we would like to verify that such shorts will not disturb the dark current in areas other than their own location on the target. This is perhaps most easily verified by referring to the equivalent circuit of Figure 3, Appendix A. If r_D is a short, the voltage V_{TM} must equal V, the mesh to Si voltage at all times. Therefore the capacitance C_{MT} cannot pass any current during the frame time and the shorted diode should only contribute to the signal during the read time. Such a shorted diode would then pass a current given by

$$i_{Read}\,(\text{short}) = (\delta-1)\,i_b + \frac{V}{r_b} \tag{15}$$

during the read time, and

$$i_{Stored}\,(\text{short}) = 0 \tag{16}$$

during the frame time. If we examine equation (25) of Appendix A, it is clear that if the capacitor C_{TM} were discharging significantly during the frame time, for the average diode of the target, then the short would not contribute to this integral properly, so that the integral would not be precisely zero. However for high impedance diodes in the dark, none of the diodes will change their state significantly during the frame time, and $C_{TM}\,\frac{d\,V_{TM}}{dt}$ will be approximately zero for all diodes independently during the time that we are not reading them. Therefore the integral will not be disturbed appreciably in the dark. This would not be the case for a uniform background of photon flux as discussed in Section 3.

3. Fluctuations in Photoresponse for a Uniform Background Flux

Let us assume that the vast majority of the diodes have an impedance r_D which is high enough that the dark current in the storage mode is unimportant. Then the equivalent circuit of Appendix A is a great deal simpler to analyze. If a uniform photon flux falls on the diodes, the average diode would then be contributing a current to the signal given by

negative mode of high beam velocity operation) by an amount

$$V_{FT} = \overline{V}\, \ell n\delta$$

where $\overline{V}$ = average energy of secondaries from metal island and SiO_2

δ = average secondary emission yield

The oxide surface will track the potential of the metal islands as a result of redistribution of secondary electrons and beam induced conductivity, while being opaque to the normal flow of beam electrons as a result of space charge buildup.

The reverse impedance of the metal-silicon Schottky barriers will be unaffected by surface inversion of the silicon under the silicon dioxide. It will, however, be degraded by oxide field induced barrier lowering at the perimeter of the metal-silicon contact. This phenomena, if present, would be similar to that observed when a number of metal islands (and the intervening oxide) are over-coated with metal to permit diode I-V measurements. In this case, barrier lowering is evidenced by large values of the diode ideality factor n in the forward direction.

B. Uniformity in Tube Response

The importance of uniformity in the response of the camera tube has been recognized by Hall and Dimmock [8], [9], who show that if the background signal can be removed prior to readout, the usefulness of a camera tube can be extended further into the infrared. The extent to which one can remove the background is limited by the uniformity of the tube response to the background.

This fact makes Schottky diodes appear particularly attractive since they are majority carrier devices, and their photoelectric response depends primarily on the metal-semiconductor interface and the absorption in the metal. As discussed by Shepherd and Yang [1], such properties as lifetime, resistivity, and capacitance in the semiconductor should have little to no effect on the photoelectric yield. The correctness of this basic assumption has been in fact experimentally verified by Shepherd and Yang [1] who show a much more uniform response of a large area Schottky diode to light at wavelengths longer than the Si band edge than to light in the visible. In the latter case, the device would respond as a minority carrier device and reflect the variations of the Si parameters.

In addition to the photoelectric yield, the response of the tube can be affected by the uniformity of the various parameters entering into the equivalent circuit of Figure 3 (Appendix A). In Section 3 below, we will take each of these parameters γ, r_b, r_D, C_{TM}, C_{TS}, δ, i_b and t_R; and discuss how variations in them will affect the response of the tube to a uniform photon flux. Before doing this, however, we define in Section 1 the dynamic range of the tube. This helps us to determine the level of fluctuations which are important to us. In Section 2 we discuss the parameters that will affect the fluctuations in the dark current in the absence of a photo flux.

1. Dynamic Range of Tube

It is clear that there is a maximum current of electrons which can be carried away from the target under the influence of the electron beam. This current is given by

$$I_{s_{max}} = m(\delta-1) i_b \tag{11}$$

where the symbols are those used in Appendix A. Since δ goes through a maximum with increasing cathode to target voltage, this current will have a maximum at some landing voltage. For the experimental tubes used to date, this maximum current has been $\lesssim$ 200 na, and it is not likely that changes in tube design would increase this number significantly, since, n_{ib}, the beam current, is limited to $\approx$ 1 μamp.[8] On the other hand, the noise current in the state of the art 4.5 MHz preamp is given by Hall as 2 na.[8] Therefore there is a current range of a factor of about 100 that we can measure with the tube, whether this current be dark current, background photocurrent, or true signal photocurrent, or the sum of all three. Ideally we would like the average dark current as well as its mean square fluctuations measured over the tube to be less than the 2 μamps of noise current from the preamp. In this case the dark current would not degrade the already limited dynamic range of the tube. Schemes for the removal of the average background and dark current have been suggested (e.g. the flood beam approach of Dimmock[9]). If there are spatial deviations in the current however, these spatial deviations from the mean could not be easily removed and would be left to reduce the dynamic range.

If the tube is operating in the full storage mode, the average dark current due to diode leakage would be given by

$$i_{s_{Read}} = \left(1 - \frac{C_{TM}}{C}\right)\left(yi_{ph}\right)\left(\frac{t_f - t_R}{t_R}\right) \tag{17}$$

during the read time and

$$i_{s_{Stored}} = 1 - \frac{C_{TM}}{C} \quad (yi_{ph}) \tag{18}$$

during the storage time. If all diodes are behaving in this manner, the total signal being read is

$$I_s = \sum_N i_s$$

$$= yi_{ph}\left[n\left(1 - \frac{C_{TM}}{C}\right)\left(\frac{t_f - t_R}{t_R}\right) + \frac{C_{TM}}{C}\left(N-n\right)\right] \tag{19}$$

where n is the number of diodes being read at any given time. Since

$$\left(\frac{N-n}{n}\right) = \frac{t_f - t_R}{t_R} \tag{20}$$

equation (17) is given by

$$I_s = n\ yi_{ph}\left(\frac{t_f - t_R}{t_R}\right) \tag{21}$$

when all diodes are uniform.

We will now discuss deviations from this average current (Cf. eq. 21) for a diode which has properties different than the average diode.

First let us consider r_D. In the worst case $r_D = 0$ for a particular diode. Then that diode would contribute the currents in (15) and (16) to the summation in (19) rather than the currents in (17) and (18). Therefore the change in photosignal when the short is being read

$$\Delta I_{s_{Read}} = \left[(\delta-1)\, i_b + \frac{V}{r_b}\right] - \left[\left(1 - \frac{C_{TM}}{C}\right)\ yi_{ph}\left(\frac{t_f - t_R}{t_R}\right)\right] \tag{22}$$

and the change in photosignal when the short is not being read is

$$\Delta I_{s_{Stored}} = - \frac{C_{TM}}{C}\ yi_{ph} \tag{23}$$

Therefore it there is a short, the background would look a little darker when the short is not under the beam than it would if there were no short. While the short is being read, the change in signal due to the short could either be positive or negative depending on whether the dark current which the short is passing is larger or smaller than the photocurrent it would have passed if it were not a short. Therefore for low background fluxes we would read the short as a bright spot. For high background fluxes we would read a short as a dark spot. For fluctuations in r_D around some high value, equations (17) and (18) will be unaffected. Therefore except for points where r_D fails catastrophically it should not contribute to fluctuations in the photosignal.

Equations (17) and (18) show that if C_{TM}/C is $\ll 1$ where $C = C_{TM} + C_{TS}$, the values of the capacitance drop out of the response. However equations (17) and (18) show clearly that C_{TM}/C must be much less than unity in order to take full advantage of the storage mode gain. This is because C_{TM} is being discharged through the output signal path during the entire frame time, and is not being changed through the output signal during the read time. It is therefore affecting the signal in exactly the opposite way from C_{TS}. While C_{TM}/C_{TS} must be made small enough that it does not seriously affect the average signal, nonetheless, fluctuations in the capacitance can cause fluctuations in the signal.

The signal from a particular diode may be rewritten as

$$i_{s\ \text{Read}} \quad \left(\frac{C_{TS}}{C_{TM} + C_{TS}} \right) y i_{ph} \quad \left(\frac{t_f - t_R}{t_R} \right) \tag{24}$$

during the read time. Let

$$C_{TS} = \langle C_{TS} \rangle + \Delta C_{TS} \tag{25}$$

and

$$C_{TM} = \langle C_{TM} \rangle + \Delta C_{TM} \tag{26}$$

where $\langle C_{TS} \rangle$ and $\langle C_{TM} \rangle$

denote average values over the retina surface. Then if a particular diode with a ΔC_{TS} and ΔC_{TM} is being read,

$$\Delta I_{s_{Read}} = \frac{yi_{ph}\left(t_f - t_R\right)}{t_R\left\langle C_{TM} + C_{TS}\right\rangle}\left[\frac{\left\langle C_{TM}\right\rangle \Delta C_{TS} - \left\langle C_{TS}\right\rangle \Delta C_{TM}}{\left\langle C_{TM}\right\rangle + \Delta C_{TM} + \Delta C_{TS}}\right] \quad (27)$$

This may be approximated by

$$\Delta I_{s_{Read}} \approx \left\langle I_s\right\rangle \frac{\left\langle C_{TM}\right\rangle}{\left\langle C_{TM} + C_{TS}\right\rangle}\left(\frac{\Delta C_{TS}}{\left\langle C_{TS}\right\rangle} - \frac{\Delta C_{TM}}{\left\langle C_{TM}\right\rangle}\right) \quad (28)$$

if fluctuations in C_{TM} and C_{TS} are not too large compared to their average values. If the percentage fluctuations in C_{TM} are equal to the percentage fluctuations in C_{TS}, they will both cause equal fluctuations in the signal. Regions of high capacitance in C_{TS} would look brighter than average, while regions of high capacitance in C_{TM} would look darker than the average. Fluctuations in C_{TS} can be expected to occur if there are fluctuations in the resistivity of the Si. A wavy mesh could cause large fluctuations in C_{TM} over broad areas of the target. For example the center of the target may have a higher C_{TM} than the periphery. Such broad scale fluctuations, would be more detrimental than an occasional random fluctuation in the resistivity of the Si which would appear as a cosmetic defect in the picture. This suggests that the integrated mesh would be a good way to go. However this would increase the factor $\frac{C_{TM}}{C_{TM} + C_{TS}}$ which multiplies ΔI_s. Furthermore $\left(\frac{\Delta C_{TM}}{C_{TM}}\right)$ may still vary significantly if the spacing between the edge of the integrated mesh and the metal diode varies, since C_{TM} is a fringing capacitance. Fluctuations in the capacitances would thus tend to reflect directly in the signal to the degree that $\frac{C_{TM}}{C_{TM} + C_{TS}}$ differs from 0.

On the other hand, if C_{TM} is made too small, redistribution of the secondaries will come into play, and degreade the resolution of the picture. Therefore there should be an optimum in C_{TM} for overall tube performance.

If $(\delta-1)i_b$ varies from spot to spot, it will not affect the output unless it fails below $yi_{ph}\left(\frac{t_f - t_R}{t_R}\right)$. Then the dynamic range of that particular spot would be

reduced below the background and it would appear as a dark spot compared to the rest of the tube.

r_b, the beam impedance predominately enters to determine the speed of response of the tube, without affecting the integrated current during the read time once we have reached a cyclic state. Therefore for stationary pictures it should have little to no effect on the signal current.

The photoelectric yield y, enters linearly into the signal. Therefore percentage fluctuations in it would be reflected directly in the response of the tube.

The photosignal is also directly proportional to $m\left(\frac{t_f - t_R}{t_R}\right)$, so that percentage fluctuations in n/t_R will appear as percentage fluctuations in the output. If the beam is focused more at one spot on the tube than it is on another, the read time would vary as we move across the tube. However the number of diodes which we are reading would also vary in proportion to t_R, and this would not cause fluctuations in the response of the tube. On the other hand if one particular diode is read more than once during the frame time because the beam overlaps itself as it scans, this would affect t_R without affecting n and cause fluctuations in the output. Therefore irregularities in the amount that the beam overlaps itself can occur as a result of the fact that the beam is not focused by the same amount at all points in the tube. There could thus be large scale fluctuations in the amplification factor as a result of the electronics of the scanning.

4. Conclusions

If we can get $(\delta-1)\, i_b$, r_b and r_D in the ranges that theory predicts, fluctuations in these values should not affect the output signal from a uniform background. (Fluctuations in $(\delta-1)\, i_b$ will only cause fluctuations in the dynamic range of the tube, while fluctuations in r_b would only cause fluctuations in the speed of response.) Percentage fluctuations in y and $n\left(\frac{t_f - t_R}{t_R}\right)$ will cause the same percentage fluctuations in the output signal. Percentage fluctuations in the capacitors C_{TM} and C_{TS} would cause percentage fluctuations in the output signal that would be reduced by an amount $\frac{C_{TM}}{C_{TM} + C_{TS}}$.

Thus fluctuations in y, $n\left(\frac{t_f - t_R}{t_R}\right)$, C_{TM} and C_{TS} must be controlled in order to obtain response to a background that can be erased by simple techniques.

III. REFERENCES

1. F. D. Shepherd, Jr. and A. C. Yang, "Silicon Schottky Retinas for Infrared Imaging," Proc. 1973 International Electron Devices Meeting, December 1973.

2. J. P. Spratt and R. F. Schwarz, "Metal-Silicon Schottky Diode Arrays as Infrared Vidicon Retinae," Proc. 1973 International Electron Devices Meeting, December 1973.

3. J. Cohen, J. Vilms and R. J. Archer, "Investigation of Semiconductor Schottky Barriers for Optical Detection and Cathodic Emission," Final Report, Contract No. F19628-68-C-0090, 18 December 1968.

4. J. Dresner, "The High Beam Velocity Vidicon," RCA Review, Vol. XXII, pp. 305-324, June 1961.

5. J. P. Spratt, "Infrared Vidicon Development," Final Report, Contract No. F19628-73-C-0221, Air Force Cambridge Research Labs.

6. S. M. Sze, "Physics of Semiconductor Devices," Wiley-Interscience, (1969), p. 468.

7. Op. cit, p. 421.

8. J. A. Hall, Applied Optics, 10, No. 4, p. 838, April 1971.

9. J. O. Dimmock, Lincoln Laboratory Technical Note, 1971-49, 3 December 1971.

10. C. R. Crowell and R. M. Madden, "Large Signal Transient Analysis and Effects of Laterla Charge Spreading in Television Camera Tubes," IEE Transactions on Electron Devices, Vol. ED. 18, pp. 1049-1057, November, 1971.

APPENDIX A

ANALYSIS OF AN EQUIVALENT CIRCUIT FOR A HIGH BEAM VELOCITY VIDICON EMPLOYING SECONDARY EMISSION

I.A Introduction

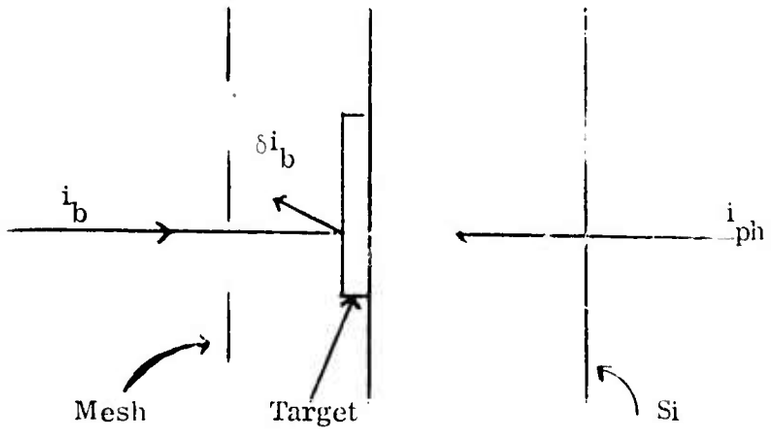

Figure A1

Schematic diagram of a Schottky diode under bombardment by an electron beam, i_b

A schematic diagram of a Schottky diode representing a single element in the vidicon is shown in Figure A1. It is being bombarded by an electron beam of current, i_b, entering the mesh from the cathode. This beam is assumed to generate δi_b secondaries where δ is greater than 1. The number of these secondaries which can escape to the mesh is determined by the target to mesh voltage, V_{TM}. If the secondaries are assumed to have a Maxwellian energy distribution with an average energy $\overline{V}$, then the current of secondary electrons which can escape to the mesh is given by

$$i_{sec_{TM}} = \delta i_b e^{\frac{-V_{TM}}{\overline{V}}} \tag{1A}$$

Of these, i_b, will be equal and opposite to the primary beam flowing to the target from the cathode. There thus appears to be a current of electrons, i_b, flowing from cathode to mesh, and a net positive current flow from target to mesh given by

$$i_{TM} = i_b - \delta i_b e^{\frac{-V_{TM}}{\overline{V}}}$$

$$= i_b (\delta - 1) + \delta i_b \left(1 - e^{\frac{-V_{TM}}{\overline{V}}}\right) \tag{2A}$$

The current in the first term on the right of equation (2A) is independent of the target to the mesh voltage and behaves like a current generator driving a positive current from mesh to target if δ is greater than 1. The second term on the right of equation (2A) represents a current controlled by the target to mesh voltage. This is describable in an equivalent circuit by a voltage dependent resistor, r_b, in parallel with the current generator described by the first term. For a Maxwellian energy distribution, r_b is by definition

$$1/r_b \equiv \frac{d\left\{\delta i_b \left(1 - e^{\frac{-V_{TM}}{\bar{v}}}\right)\right\}}{dV_{TM}}$$

$$= \frac{\delta i_b}{\bar{v}} e^{\frac{-V_{TM}}{\bar{v}}} \qquad (3A)$$

There is also a target to mesh capacitance, C_{TM}, in parallel with r_b and the current generator i_b (δ-1). An equivalent circuit for the particular element shown in Fig. A1, may thus be described by Fig. A2. Here the diode is represented by the parallel combination of a resistance r_D, a capacitance C_{TS}, and a current generator, yi_{ph} where i_{ph} is the photon flux on the diode, and y is the responsivity of the diode in amps/watt.

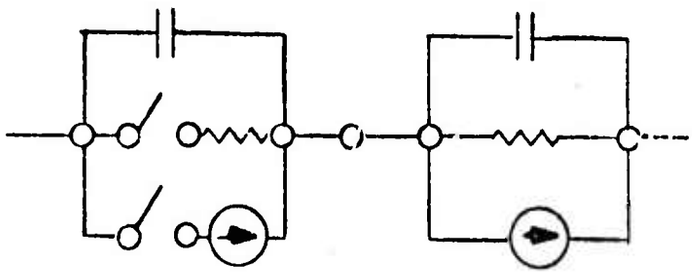

Figure A2

Equivalent circuit for the element

in Figure A1

The switches in the mesh to target loop are closed during the read time, t_r, when the electron beam is on the diode, and are open during the remainder of the frame time, $t_f - t_r$, which we shall refer to as the storage time.

If in the steady state, no current were flowing out the Si, the current, $(\delta-1)i_b$, would flow through the resistance r_b, and the voltage V_{TMo} would be determined from (2A) as

$$i_b(\delta-1) = \delta i_b\left(1 - e^{\frac{-V_{TMo}}{\bar{v}}}\right)$$

which yields

$$V_{TMo} = \bar{v}\ell n\,\delta \tag{4A}$$

In the operation of the tube,

$$0 \lesssim V_{TM} \lesssim V_{TMo} \tag{5A}$$

Thus from equations (3A), (4A) and (5A)

$$\frac{\bar{v}}{\delta i_b} \lesssim r_b \lesssim \frac{\bar{v}}{i_b} \tag{6A}$$

For δ not too different from unity, r_b does not vary appreciably over the operating range of the tube, and the equivalent circuit of Fig. A2 is conceptually quite useful. r_D and C_{TS} will both be voltage dependent, but these dependences are reasonably well understood and will be ignored in this analysis.

If there are a total of N diodes on the target, the equivalent circuit of the mesh to Si loop is represented by N loops like Ftg. A2 in parallel, plus a mesh to Si capacitance, C_{MS} also in parallel with these loops. Thus the entire mesh to Si circuit appears as shown in Fig. A3.

For this report the elements in all N loops are considered identical. A subsequent report will treat the problem of nonuniformities in the various parameters in the N loops of Fig. A3. This report also considers only the case of a short circuit load. A subsequent report will treat the problem of how the load between mesh and Si affects the signal current. A D.C. bias voltage V, between mesh and Si will be included as it does not complicate the solutions significantly.

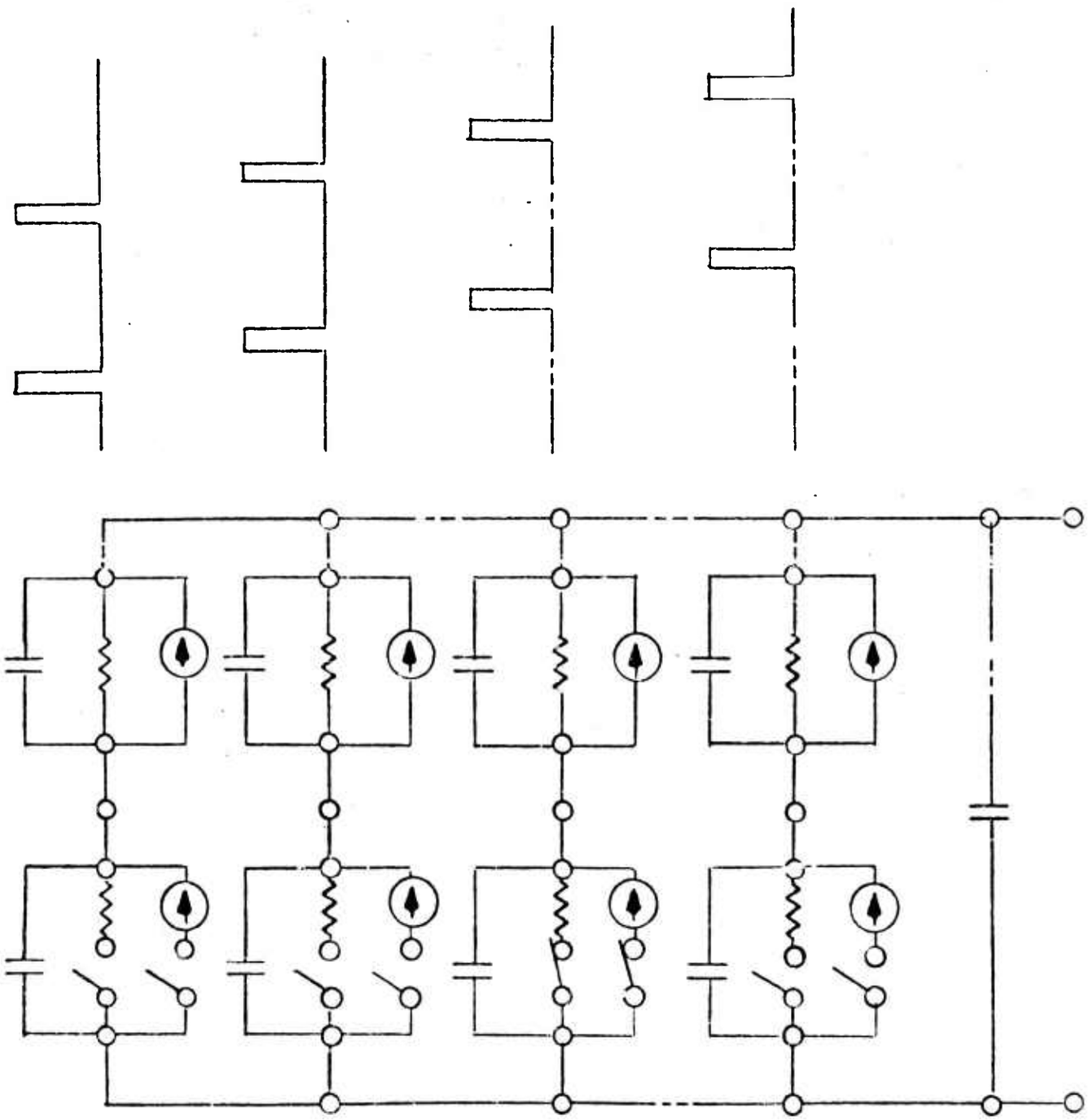

Figure A3

Entire equivalent circuit between Mesh and Si

With the above assumptions, we attempt to solve the following three problems for the output signal current; (Problem 1) Uniform light level, i_{ph}, over the entire target, no spatial or time variations occurring.

(Problem 2) an arbitrary spatial pattern of i_{ph}, over the N devices, but no time variations on any of the diodes.

(Problem 3) All diodes are uniform in i_{ph} for $t < o$. For $t \geq o$, one particular diode change to $i_{ph} + \Delta i_{ph}$. The subsequent time dependence of the output signal is calculated.

First, however, general equations which are useful to all three problems will be solved.

II.A General Equations

The component of current flowing in the output loop from any particular diode is

$$i_s = (\delta-1)\, i_b - C_{TM} \frac{d\, V_{TM}}{dt} - \frac{V_{TM}}{r_b}$$

$$= yi_{ph} + \frac{V_{TS}}{r_D} + C_{TS} \frac{d\, V_{TS}}{dt} \qquad (7A)$$

when the switch is closed, and

$$i_s = -C_{TM} \frac{d\, V_{TM}}{dt} = yi_{ph} + \frac{V_{TS}}{r_D} + C_{TS} \frac{d\, V_{TS}}{dt} \qquad (8A)$$

when the switch is open. In addition, we have for the short circuit load that

$$V_{TM} = V_{TS} - V \qquad (9A)$$

where V is any D.C. biasing voltage between mesh and Si. Here V is taken as positive if the mesh lead is positive with respect to the Si.

Combining (9A) with (7A) and (8A), we have the following differential equations for V_{TM} as a function of time.

$$\frac{V_{TM}}{r_{11}} + \frac{C\, dV_{TM}}{dt} = (\delta-1)\, i_b - \frac{V}{r_D} - yi_{ph} \qquad (10A)$$

when the switch is closed, and $\frac{V_{TM}}{r_D} + \frac{C\, dV_{TM}}{dt} = -\left(\frac{V}{r_D} \quad yi_{ph}\right)$ (11A)

when the switch is open. r_{11} is the parallel combination of r_b and r_D and C is the parallel combination of C_{TM} and C_{TS}. Thus,

$$\left.\begin{aligned} 1/r_{11} &= 1/r_b + 1/r_D \\ \text{and,}\quad C &= C_{TM} + C_{TS} \end{aligned}\right\} \qquad (12A)$$

Solutions to (10A) and (11A) are

$$V_{TM} = \left[V_{TM_o} - r_{11}\left\{(\delta-1)\, i_b - \frac{V}{r_D} - yi_{ph}\right\}\right] e^{-t/C r_{11}} + r_{11}\left\{(\delta-1)\, i_{ph} - \frac{V}{r_D} + yi_{ph}\right\} \qquad (13A)$$

when the switch is closed, and

$$V_{TM} = \left[V_{TM_R} + r_D\left(\frac{V}{r_D} + yi_{ph}\right)\right] e^{-\frac{t - t_R}{C\, r_d}} - r_D\left(\frac{V}{r_D} + yi_{ph}\right) \quad (14A)$$

when the switch is open. In equations (13A) and (14A), V_{TM_O} and V_{TM_R} represent the voltages at the beginning and end of the read time, respectively.

If the light level on the diode is independent of time, then the diode will go into a cyclic state, so that its voltage at the beginning of each read time is always the same. Then V_{TM_R} will be determined by (13A) when $t = t_R$ and V_{TM_O} will be determined by (14A) when t equals t_f. Thus V_{TM_R} and V_{TM_O} are defined for the cyclic state by the following two simultaneous equations.

$$V_{TM_R} = \left[V_{TM_O} - r_{11}\left\{(\delta-1)\, i_b - \frac{V}{r_D} - yi_{ph}\right\}\right] e^{-t_R/C\, r_{11}} + r_{11}\left\{(\delta-1)\, i_b - \frac{V}{r_D} - yi_{ph}\right\} \quad (15A)$$

and

$$V_{TM_O} = \left[V_{TM_R} + r_D\left(\frac{V}{r_D} + yi_{ph}\right)\right] e^{\frac{-t_f - t_R}{C\, r_D}} - r_D\left(\frac{V}{r_D} + yi_{ph}\right) \quad (16A)$$

Solutions to (15A) and (16A) are

$$V_{TM_R} = \left[\frac{r_{11}\left\{(\delta-1)\, i_b - yi_{ph} - \frac{V}{r_D}\right\}}{\left\{1 - e^{\frac{-(t_f - t_R)}{C\, r_D}}\right\}} - \frac{r_D\left\{yi_{ph} + \frac{V}{r_D}\right\} e^{-t_R/C\, r_{11}}}{\left\{1 - e^{-t_R/C\, r_{11}}\right\}}\right] f \quad (17A)$$

and

$$V_{TM_O} = \left[\frac{r_{11}\left\{(\delta-1)\, i_b - yi_{ph} - \frac{V}{r_D}\right\} e^{\frac{-t_f - t_R}{C\, r_D}}}{\left\{1 - e^{\frac{-t_f - t_R}{C\, r_D}}\right\}} - \frac{r_D\left(yi_{ph} + \frac{V}{r_D}\right)}{\left\{1 - e^{-t_R/C\, r_{11}}\right\}}\right] f \quad (18A)$$

where

$$f = \frac{\left(1 - e^{-t_R/C r_{11}}\right)\left(1 - e^{-\frac{(t_f - t_R)}{C r_D}}\right)}{1 - e^{-\{t_R/C r_{11} + (t_f - t_R)/C r_D\}}} \tag{19A}$$

From (13A) and (14A) it can be seen that if the switch were opened indefinitely the voltage V_{TM} would go to a value $-r_D\left(yi_{ph} + \frac{V}{r_D}\right)$, while if the switch were closed, V_{TM} would approach $r_{11}\left[(\delta-1)\, i_b - yi_{ph} - \frac{V}{r_D}\right]$. From (17A) and (18A) it can be seen that

$$V_{TM_R} - V_{TM_O} = \left[r_{11}\left\{(\delta-1)\, i_b - yi_{ph} - \frac{V}{r_D}\right\} + r_D\left\{yi_{ph} + \frac{V}{r_D}\right\}\right] f \tag{20A}$$

Therefore, f represents the fraction of the equilibrium voltage difference between the open and closed states, that the device actually swings through when it is in the cyclic state.

(17A) and (18A) may be combined with (13A) and (14A) to give the time dependence of V_{TM} when the device is in the cyclic state. Thus,

$$V_{TM} = r_{11}\left\{(\delta-1)\, i_b - yi_{ph} - \frac{V}{r_D}\right\} - \frac{\left[r_{11}\left\{(\delta-1)\, i_b - yi_{ph} - \frac{V}{r_D}\right\} + r_D\left(yi_{ph} + \frac{V}{r_D}\right)\right] f\, e^{-t_R/C r_{11}}}{\left\{1 - e^{-t_r/C r_{11}}\right\}} \tag{21A}$$

when the switch is closed, and

$$V_{TM} \left[\frac{\left[r_{11}\left\{(\delta-1)\, i_b - yi_{ph} - \frac{V}{r_D}\right\} + r_D\left(yi_{ph} + \frac{V}{r_D}\right)\right] f\, e^{-\frac{(t - t_R)}{C r_D}}}{\left\{1 - e^{-(t_f - t_R)/C r_D}\right\}}\right] - r_D\left(yi_{ph} + \frac{V}{r_D}\right) \tag{22A}$$

when the switch is open.

In summary, equations (13A) and (14A) give the time dependence of V_{TM} for arbitrary initial voltages, and equations (21A) and (22A) give the time dependence of V_{TM} when the device is in a cyclic state.

III.A Problem 1

Uniform light level over the entire target for times long enough to establish the cyclic state.

From equations (7A) and (8A), the total signal current is given by

$$I_s = n(\delta-1)\, i_b - \sum_n \frac{V_{TM}}{r_b} - \sum_N C_{TM} \frac{d V_{TM}}{dt} \tag{23A}$$

where n = number of devices being read at any given time and N equals the total number of devices on the target.

If n is large compared to (1), then

$$\sum_n \frac{V_{TM}}{r_b} \approx \frac{n}{t_R} \int_0^{t_R} \frac{V_{TM}(t)\, dt}{r_b} \tag{24A}$$

and

$$\sum_N C_{TM} \frac{d V_{TM}}{dt} \approx \frac{N}{t_f} \int_0^{t_f} C_{TM} \frac{d V_{TM}}{dt}\, dt = 0 \tag{25A}$$

for the cyclic state.

Therefore, I_s is given by

$$I_s = n(\delta-1)\, i_b - \frac{n}{t_R} \int_0^{t_F} \frac{V_{TM}(t)\, dt}{r_b} \tag{26A}$$

Combining (26A) and (21A) we obtain the average signal current being read. Thus,

$$I_s \quad n\left[\frac{r_{11}}{r_D}(\delta-1)\, i_b + \left(1 - \frac{r_{11}}{r_D}\right)\left\{y i_{ph} + \frac{V}{r_D}\right\}\right]$$

$$\cdot\left[1 + \frac{C}{t_R}(r_D - r_{11})\, f\right] \tag{27A}$$

or in terms of r_b and r_D, we have,

$$I_s = n\left[\frac{r_b}{r_b + r_D}(\delta-1)i_b + \frac{r_b}{r_b + r_D}\left\{yi_{ph} + \frac{V}{r_D}\right\}\right] \cdot\left[1 + \frac{r_D}{r_b}\quad\frac{C_{r_{11}}}{t_R}\quad f\right] \tag{28A}$$

The first term in the first square bracket on the right of (28A) represents leakage of the current generator through the diode impedance r_D, the second term represents the desired photo-current, and the third term represents additional leakage through the diode due to the bias voltage V.

It is interesting to note that

$$\frac{1\,d\,I_s}{n\,d\,(\delta-1)\,i_b} = \frac{r_b}{r_b + r_D}\left[1 + \frac{r_D}{r_b}\quad\frac{Cr_{11}}{t_R}\quad f\right] \tag{29A}$$

$$\frac{d\,I_s}{n\,d\,(yi_{ph})} = \frac{r_D}{r_b + r_D}\left[1 + \frac{r_D}{r_b}\quad\frac{Cr_{11}}{t_R}\,f\right] \tag{30A}$$

$$\frac{1\,d\,I_s}{n\,d\,V} = \frac{1}{r_b + r_D}\left[1 + \frac{r_D}{r_b}\quad\frac{Cr_{11}}{t_R}\,f\right] \tag{31A}$$

Therefore, the ratio of (29A) over (31A) would yield r_b independent of the other parameters of the system. If we operate in the constant dwell case, f is zero. Then

$$\left.\begin{aligned}\frac{1\,d\,I_s}{n\,d\,(\delta-1)\,i_b} &= \frac{r_b}{r_b + r_D}\\ \frac{1\,d\,I_s}{n\,d\,(yi_{ph})} &= \frac{r_D}{r_b + r_D}\end{aligned}\right\} \tag{32A}$$

and

$$\frac{1\,d\,I_s}{n\,d\,V} = \frac{1}{r_b + r_D}$$

The factor $\left[1 + \frac{r_D}{r_b} \frac{Cr_{11}}{t_R} f\right]$ represents the amplification of the terms in (32A) as a result of scanning. We define this factor as A, the amplification factor. Thus,

$$A = 1 + \frac{r_D}{r_b} \frac{Cr_{11}}{t_R} f$$

$$= 1 + \frac{r_D}{r_b} \left(\frac{C r_b}{t_R}\right)\left(\frac{r_D/r_b}{1 + r_D/r_b}\right)$$

$$\left[\frac{\left(1 - e^{\frac{-t_R}{C_{rb}}\left(\frac{r_D/r_b + 1}{r_D/r_b}\right)}\right)\left(1 - e^{\frac{-t_R}{C_{rb}}\left(\frac{t_f - t_R}{t_R}\right)\frac{r_b}{r_D}}\right)}{\left(1 - e^{\left(\frac{-t_R}{C_{rb}}\left(\frac{r_D/r_b + 1}{r_D/r_b}\right) + \frac{t_R}{C_{rb}}\left(\frac{t_f - t_R}{t_R}\right)\frac{r_D}{r_b}\right)}\right)}\right] \quad (33A)$$

A is thus determined by the three parameters, $t_R/C\ r_b$, $\frac{t_f - t_R}{t_R}$, and r_D/r_b. r_b, $t_R/C\ r_b$ and $(t_f - t_R)/t_R$ should be relatively insensitive to temperature. On the other hand, r_D should vary dramatically with temperature. It is therefore, interesting to study the amplification factor as a function of r_D/r_b, since r_D/r_b can be easily varied in the lab. A is plotted in Figure A4 as a function of r_D/r_b, for $\left(\frac{t_f - t_R}{t_R}\right) = 10^5$, and $t_R/C\ r_b = 0.1$, 1 and 10. The parameter $t_R/C\ r_b$ can also be varied in the lab by varying r_b. It can be seen that A can be approximated by

$$A \approx 1 + \frac{r_D}{r_b} \left(\frac{C r_b}{t_R}\right)\left(1 - e^{-t_R/C\ r_b}\right) \quad (34A)$$

for $$0 \sim \frac{r_D}{r_b} \sim \left(\frac{t_f - t_R}{t_R}\right) \frac{t_R}{C r_b} \left(\frac{1}{1 - e^{-t_R/C\ r_b}}\right) \quad (35A)$$

and $$A \approx 1 + \frac{r_D/r_b}{1 + r_D/r_b} \frac{(t_f - t_R)}{t_R} \quad (36A)$$

FIGURE A4

Vidicon Amplification Factor vs. Normalized Retina Impedance

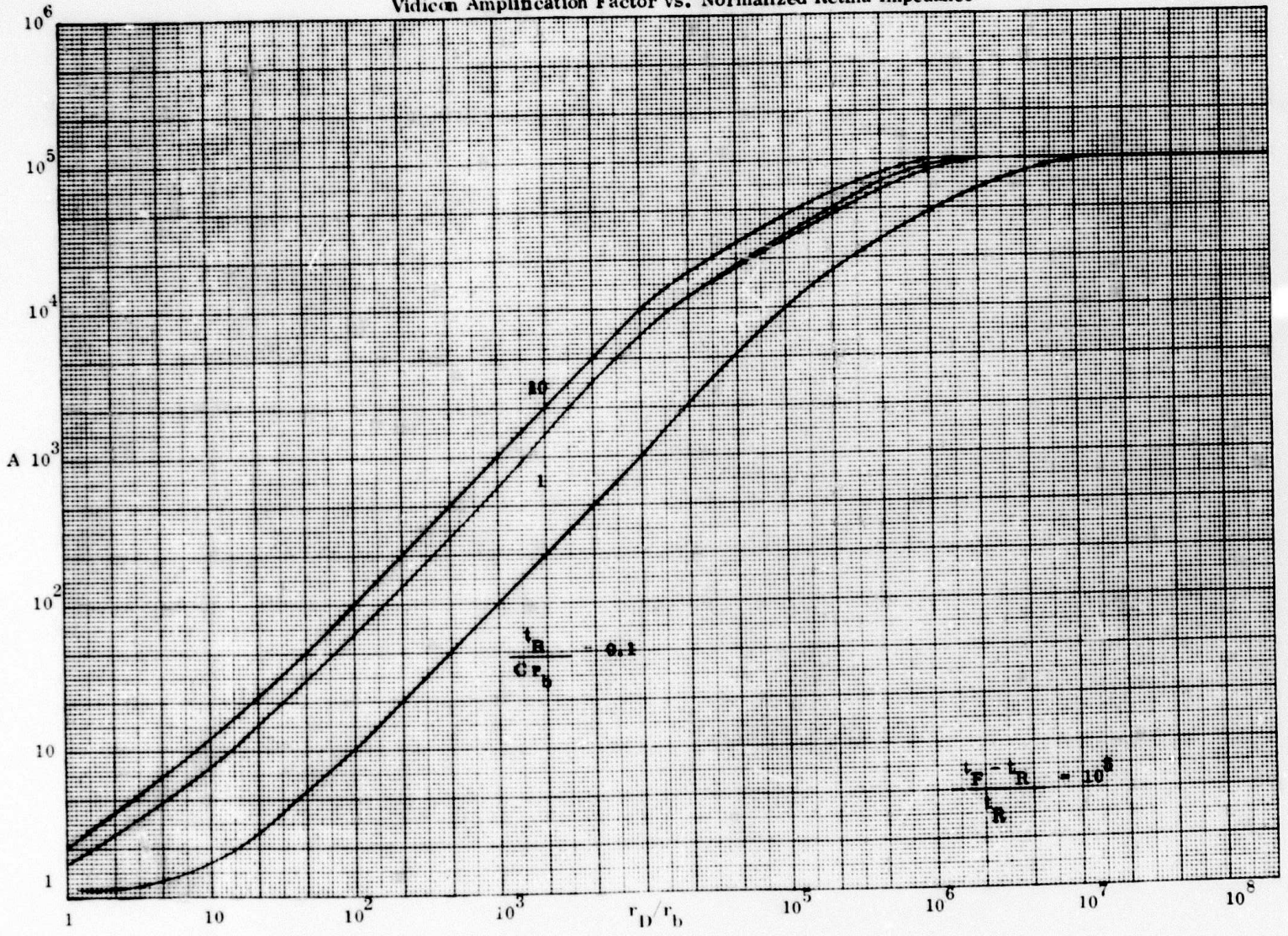

for

$$r_D/r_b \gtrsim \left(\frac{t_f - t_R}{t_R}\right) \frac{t_R}{C\, r_b} \quad \frac{1}{\left(1 - e^{-t_R/C\, r_b}\right)} \tag{37A}$$

Scanning thus results in an amplification of the photocurrent for

$$\frac{r_D}{r_b} \gtrsim \frac{t_R}{C\, r_b} \quad \frac{1}{1 - e^{-t_R/C\, r_b}} \tag{38A}$$

However the full amplification achievable in storage mode operation is not obtained until (37A) is satisfied.

Figure A5 shows $A/\left(1 + r_D/r_b\right)$ for the same parameters as Figure A4. This represents the fraction of the current generator $(\delta-1)\, i_b$ which is measured in the output loop. For $t_R/C\, r_b \lesssim 1$, the entire current generated appears in the output loop until (37A) is satisfied. For $t_R/C\, r_b \gtrsim 1$, the fraction of the current generated which appears in the output loop falls from unity to $\approx C\, r_b/t_R$ while r_D/r_b varies from unity to $t_R/C\, r_b$. It then stays at this value until (37A) is satisfied and the full amplification has been achieved.

If room temperature measurements are made of I_s in the dark, r_D will not be large enough to go into storage mode operation. Therefore from (35A) and (28A),

$$I_s \approx n\left[(\delta-1)\, i_b + \frac{V}{r_b}\right] \cdot \left[\frac{1 + \dfrac{r_D}{r_b} \quad \dfrac{C\, r_b}{t_R}\left(1 - e^{-t_R/C\, r_b}\right)}{1 + r_D/r_b}\right] \tag{39A}$$

At room temperature r_D/r_b should be less than 1, and the second square bracket on the right of (39A) should be ≈ 1. Thus, a study of this curve at room temperature as a function of i_b and V should yield the entire secondary emission distribution as well as . It will therefore determine r_b. For decreasing temperature, r_D/r_b will increase until it reaches a value greater than 1. If t_R is made infinite, (i.e. the constant dwell case), then I_s should begin to drop as $(r_D/r_b)/(1 + r_D/r_b)^2$ for constant i_b and V.

FIGURE A5

Normalized Vidicon Dark Current vs. Normalized Retina Impedance

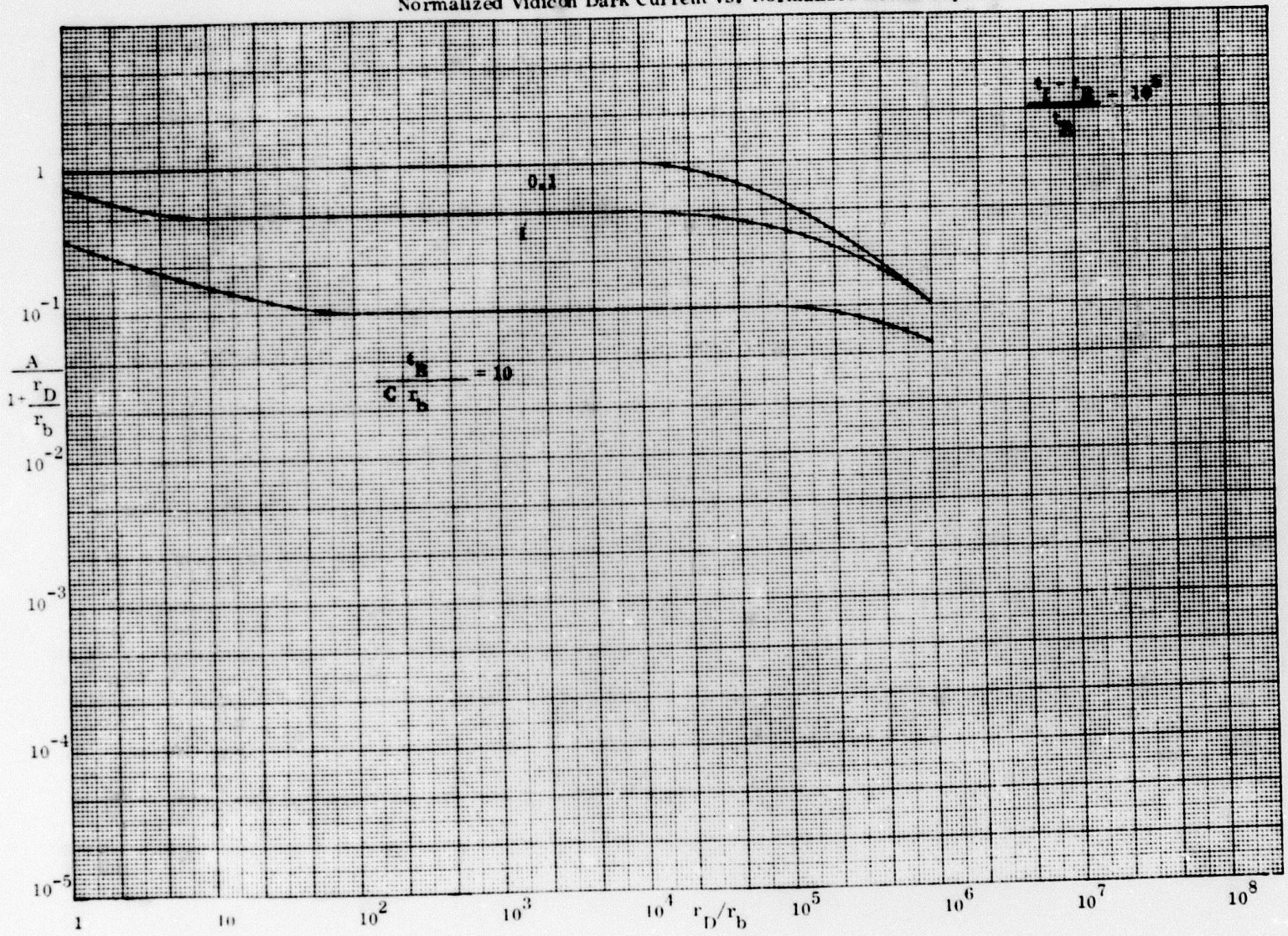

Therefore, r_D/r_b can be determined as a function of temperature from the constant dwell case. If we then scan the system, varying the parameter $t_R/C\ r_b$, (by varying i_b, for example) we will reach a value of $t_R/C\ r_b > 1$. The signal current will then drop, in accordance with (39A), by a factor of $\dfrac{t_R/C\ r_b}{1 - e^{-t_R/C\ r_b}}$ when r_D/r_b becomes greater than 1. Measurements of the two plateaus in Figure (5A) can thus yield C, the parallel capacitance of the system. As the temperature is dropped, increasing r_D/r_b still further, we will reach a region when the output current again begins to fall. This will begin to occur when (37A) is satisfied. This measurement defines the temperature at which the device must be operated for complete storage mode operation. If r_D levels off with temperature due to leakage, we may never reach this condition.

IV.A Problem 2

Arbitrary spatial pattern of i_{ph} over the N diodes, but no time variations of i_{ph} on any of the diodes.

Let the photocurrent falling on a particular diode be $\langle i_{ph} \rangle + \Delta i_{ph}$ where $\langle i_{ph} \rangle$ is the average photocurrent falling on the entire target. Then it this pattern is stationary in time, the particular diode in question is in a cyclic state, and the voltage on that particular diode may be calculated from (21A) and (22A) as

$$V_{TM} = r_{11}\left\{(\delta-1)\, i_b - y\langle i_{ph}\rangle - \frac{V}{r_D}\right\} - \frac{\left[r_{11}(\delta-1)\, i_b + (r_D - r_{11})\left(y\langle i_{ph}\rangle + \dfrac{V}{r_D}\right)\right] f\, e^{-t/C\, r_{11}}}{1 - e^{-t_R/C\, r_{11}}} - y\Delta i_{ph}\left[r_{11} + \frac{(r_D - r_{11})\, f\, e^{-t/C\, r_{11}}}{1 - e^{-t_r/C\, r_{11}}}\right] \tag{40A}$$

during the read time and

$$V_{TM} = \frac{\left[r_{11}(\delta-1)\, i_b + (r_D - r_{11})\left(y\langle i_{ph}\rangle + \frac{V}{r_D}\right)\right] f\, e^{\frac{-(t - t_R)}{C\, r_D}}}{1 - e^{-(t_f - t_R)/C\, r_D}}$$

$$- r_D\left(y\langle i_{ph}\rangle + \frac{V}{r_D}\right)$$

$$+ y\,\Delta i_{ph}\left[\frac{(r_D - r_{11})\, f\, e^{\frac{-(t - t_R)}{C\, r_D}}}{1 - e^{\frac{-(t_f - t_R)}{C\, r_D}}} - r_D\right] \qquad (41A)$$

during the frame time.

Equations (40A) and (41A) show that ΔV_{TM}, the change in the voltage, V_{TM}, due to the change in photocurrent Δi_{ph} is

$$\Delta V_{TM} = -y\,\Delta i_{ph}\left[r_{11} + \frac{(r_D - r_{11})\, f\, e^{-t/C\, r_{11}}}{\left(1 - e^{-t_R/C\, r_{11}}\right)}\right] \qquad (42A)$$

during the read time, and

$$\Delta V_{TM} = y\Delta i_{ph}\left[\frac{(r_D - r_{11})\, f\, e^{\frac{-(t - t_R)}{C\, r_D}}}{1 - e^{\frac{-(t_f - t_R)}{C\, r_D}}} - r_D\right] \qquad (43A)$$

during the frame time. The change in signal due to this change in voltage may be calculated from (7A) and (8A) in conjunction with (42A) and (43A).

Thus,

$$\Delta i_s = y\,\Delta i_{ph}\left(\frac{r_D - r_{11}}{r_D}\right)\left[1 + \frac{\left(\frac{r_D}{r_{11}} - 1\right) f\, e^{-t/C\, r_{11}}}{1 - e^{-t_R/C\, r_{11}}}\right]$$

$$- y \Delta i_{ph} \frac{C_{TM}}{C} \left[\left(\frac{r_D}{r_{11}} - 1 \right) \frac{f \; e^{- t/C \, r_{11}}}{1 - e^{-t_R/C \, r_{11}}} \right] \tag{44A}$$

during the read time, and

$$\Delta i_s = y \Delta i_{ph} \frac{C_{TM}}{C} \left(1 - \frac{r_{11}}{r_D} \right) \frac{f \; e^{\frac{-(t - t_R)}{C \, r_D}}}{1 - e^{\frac{-(t_f - t_R)}{C \, r_D}}} \tag{45A}$$

during the frame time.

Equation (45A) shows that due to the capacitance C_{TM} some photocurrent appears in the external circuit during the entire frame time from the particular diode being examined.

In actual practice, we are measuring signals from the various $\Delta i_{ph}(x)$ at some given time. The times in equations (44A) and (45A) may be related to x through the condition,

$$t = \frac{x}{v} = \frac{t_R x}{\ell} \tag{46A}$$

where ℓ is the dimension of the beam in the direction of motion of the beam, and v is the velocity of the beam. Thus

$$\Delta I_s = \sum_n \Delta i_s \approx$$

$$n \left(\frac{r_D - r_{11}}{r_D} \right) \int_o^{\frac{x}{e} = 1} y \Delta i_{ph} \left(\frac{x}{\ell} \right) \; d \left(\frac{x}{\ell} \right)$$

$$+ n \left(\frac{r_D - r_{11}}{r_{11}} \right) \frac{\left[\left(\frac{r_D - r_{11}}{r_D} \right) - \frac{C_{TM}}{C} \right] f}{1 - e^{-t_R/C \, r_{11}}} \int_o^{\frac{x}{e} = 1} \Delta i_{ph} \left(\frac{x}{\ell} \right) e^{- \frac{x}{\ell} \frac{t_R}{C \, r_{11}}} \; d \left(\frac{x}{\ell} \right)$$

$$+(N-n)\left(\frac{r_D - r_{11}}{r_D}\right)\frac{C_{TM}}{C}\;\frac{f\int_{1}^{\frac{N}{n}=\frac{t_f}{t_R}} y\,\Delta i_{ph}\left(\frac{x}{\ell}\right) e^{\frac{-t_R}{C r_D}\left(\frac{x}{\ell}-1\right)}\, d\left(\frac{x}{\ell}\right)}{\left(t_f/t_R - 1\right)} \qquad (47A)$$

$$1 - e^{\frac{-(t_f - t_R)}{C r_D}}$$

Since $N/n = t_f/t_R$, equation (47A) may be rewritten as

$$\Delta I_s =$$

$$\frac{n r_D}{r_D + r_b}\int_0^1 y\,\Delta i_{ph}\left(\frac{x}{\ell}\right)\left[1 + \frac{r_D}{r_b}\;\frac{f\; e^{\frac{-x}{\ell}\frac{t_R}{C r_{11}}}}{1 - e^{-t_R/C r_{11}}}\right] d\left(\frac{x}{\ell}\right)$$

$$- n\frac{C_{TM}}{C}\;\frac{r_D}{r_b}\;f\;\frac{C r_{11}}{t_R}\left[\frac{\frac{t_R}{C r_{11}}\int_0^1 y\,\Delta i_{ph}\left(\frac{x}{\ell}\right) e^{-\frac{x}{\ell}\left(\frac{t_R}{C r_{11}}\right)}\, d\left(\frac{x}{\ell}\right)}{\left(1 - e^{-t_R/C r_{11}}\right)}\right]$$

$$-\frac{t_R}{C r_D}\int_1^{t_f/t_R} \frac{y\,\Delta i_{ph}\left(\frac{x}{\ell}\right) e^{-\left(\frac{x}{\ell}-1\right)\frac{t_R}{C r_D}}\, d\left(\frac{x}{\ell}\right)}{\left(1 - e^{-(t_f - t_R)/C r_D}\right)} \qquad (48A)$$

In this expression, $x = 0$ is always at the leading edge of the beam and $\frac{x}{\ell} = 1$ is at the trailing edge. Expression (48A) may be rewritten in terms of the amplification of factor A. Thus,

$$\Delta I_s \;\frac{n r_D}{r_D + r_b}\int_0^1 y\,\Delta i_{ph}\left(\frac{x}{\ell}\right) d\left(\frac{x}{\ell}\right)$$

$$+\frac{n r_D}{r_D + r_b}\;(A-1)\int_0^1 y\,\Delta i_{ph}\left(\frac{x}{\ell}\right) e^{\frac{x}{\ell}\frac{t_R}{C r_{11}}}\;\frac{\frac{t_R}{C r_{11}}\, d\left(\frac{x}{\ell}\right)}{\left(1 - e^{-t_R/C r_{11}}\right)}$$

$$- n \frac{C_{TM}}{C} (A - 1) \int_0^1 \frac{y \Delta i_{ph} \left(\frac{x}{\ell}\right) e^{-\frac{x}{\ell} \frac{t_R}{C r_{11}}} \frac{t_R}{C r_{11}} d\left(\frac{x}{\ell}\right)}{\left(1 - e^{-t_R/C r_{11}}\right)}$$

$$- \int_1^{t_f/t_R} \frac{y \Delta i_{ph} \left(\frac{x}{\ell}\right) e^{-\left(\frac{x}{\ell} - 1\right) \frac{t_R}{C r_D}} \frac{t_R}{C r_D} d\left(\frac{x}{\ell}\right)}{\left(1 - e^{-(t_f - t_R)/C r_D}\right)} \qquad (49A)$$

For $t_R/C\, r_{11} \lesssim 1$ and $\frac{t_f - t_R}{C r_D} < 1$, this expression reduces to

$$\Delta I_s \approx \frac{n r_D}{r_D + r_b} A y \langle \Delta i_{ph} \rangle t_R$$

$$- n \frac{C_{TM}}{C} (A - 1) y \left[\langle \Delta i_{ph} \rangle t_R - \langle \Delta i_{ph} \rangle t_f - t_R \right] \qquad (50A)$$

For $C_{TM}/C \ll 1$, this result is that which would be expected of a camera tube. The resolution of the tube is in this case limited by the dimensions of the beam. For $t_R/C\, r_{11} > 1$ and $\frac{t_f - t_R}{C r_D} < 1$, (50A) may be approximated by

$$\Delta I_s \approx \frac{n r_D}{r_D + r_b} y \langle \Delta i_{ph} \rangle t_R$$

$$+ \frac{n r_D}{r_D + r_b} y (A - 1) \langle \Delta i_{ph} \rangle \left(\frac{C r_{11}}{t_R} \cdot t_R \right)$$

$$- n \frac{C_{TM}}{C} y (A - 1) \left[\frac{\langle \Delta i_{ph} \rangle}{\left(\frac{C r_{11}}{t_R} t_R \right)} - \langle \Delta i_{ph} \rangle t_f - t_R \right] \qquad (51A)$$

If this case is appropriate, the resolution is determined by $\frac{C\, r_{11}}{t_R} \times \ell$ where ℓ is the dimension of the beam in the direction of its motion. In either case, the terms in C_{TM} have the effect of giving some signal during the storage time. If there is a highlight somewhere, for example, there would be a glow during the entire storage time due to this highlight.

V.A Problem 3

Response time of the tube to a changing light level.

Let i_{ph} be uniform over all of the diodes except one. On the particular one being studied, let Δi_{ph} be applied to that diode at $t = t_o$, where t_o is the time since the beam last crossed that element. Then that particular element is not in a cyclic boundary condition, and we ask what will happen to the voltage on it as a function of time. The differential equations which define the time dependence of ΔV_{TM} are

$$y\, \Delta i_{ph} = - Cd \frac{\Delta V_{TM}}{dt} - \frac{\Delta V_{TM}}{r_{11}} \tag{52A}$$

during the read time, and

$$y\, \Delta i_{ph} = - \frac{V_{TM}}{dt} - \frac{\Delta V_{TM}}{r_D} \tag{53A}$$

during the frame time. Solutions to (52A) and (53A) are

$$\Delta V_{TM} = (\Delta V_{TM_{o_n}} + y\, \Delta i_{ph}\, r_{11})\, e^{-t/C\, r_{11}} - y\, \Delta i_{ph}\, r_{11} \tag{54A}$$

during the read time, and

$$\Delta V_{TM} = \left[(\Delta V_{TM_{o_n}} + y\, \Delta i_{ph}\, r_{11})\, e^{-t_R/C\, r_{11}} + y\, \Delta i_{ph}\, (r_D - r_{11}) \right] e^{\frac{-t - t_R}{C\, r_D}} - y\, \Delta i_{ph}\, r_D \tag{55A}$$

during the frame time. In this equation, $\Delta V_{TM_{o_n}}$ is the change in voltage on the diode as a result of Δi_{ph}, the n^{th} time that the leading edge of the beam crosses the diode after Δi_{ph} has been turned on.

A recursion relation for $\Delta V_{TM_{o_n}}$ may immediately be obtained from (55A). Thus

$$\Delta V_{TM_{o_{n+1}}} = \Delta V_{TM_{o_n}} e^{-\left(t_R/C r_{11} + \frac{t_f - t_R}{C r_D}\right)} + \Delta V_{TM_{o_\infty}} \left\{1 - e^{-\left(t_R/C r_{11} + \frac{t_f - t_R}{C r_D}\right)}\right\} \tag{56A}$$

where

$$\Delta V_{TM_{o_\infty}} = -y \Delta i_{ph} \left(r_{11} + \frac{(r_D - r_{11}) f}{1 - e^{-t_R/C r_{11}}} \right) \tag{57A}$$

(56A) may be reused repeatedly to show that

$$\Delta V_{TM_{o_{n+1}}} = \Delta V_{TM_{o_1}} e^{-n\left(\frac{t_R}{C r_{11}} + \frac{t_f - t_R}{C r_D}\right)} + \Delta V_{TM_{o_\infty}} \left(1 - e^{-\left(\frac{t_R}{C r_{11}} + \frac{t_f - t_R}{C r_D}\right)} \right) \left[1 + e^{-\left(\frac{t_R}{C r_{11}} + \frac{t_f - t_R}{C r_D}\right)} + \right.$$

$$\left. \cdots\cdots\cdots e^{-(n-1)\left(\frac{t_R}{C r_{11}} + \frac{t_f - t_R}{C r_D}\right)} \right.$$

or

$$\Delta V_{TM_{o_{n+1}}} = \Delta V_{TM_{o_1}} e^{-n\left(\frac{t_R}{C r_{11}} + \frac{t_f - t_R}{C r_D}\right)}$$

$$+ \Delta V_{TM_{o_\infty}} \left(1 - e^{-n\left(\frac{t_R}{C r_{11}} + \frac{t_f - t_R}{C r_D}\right)}\right) \qquad (58A)$$

(58A) shows that the initial voltage, $\Delta V_{TM_{o_n}}$, will appear to decay exponentially in time to its new cyclic state, with a time constant given by

$$\tau = \frac{t_f}{\left(\frac{t_R}{C r_{11}} + \frac{t_f - t_R}{C r_D}\right)} \qquad (59A)$$

(59A) defines the response time of the tube. The factor $\frac{1}{t_R/C r_{11} + \frac{t_f - t_R}{C r_D}}$ gives the approximate number of frames necessary to establish a new cyclic state once Δi_{ph} has been turned on.

The only remaining point of interest is the value of $\Delta V_{TM_{o_1}}$. This depends on the time, t_o, since the beam last crossed the element when the light, Δi_{ph}, was turned on. Its value may be calculated from (54A) and (55A) as

$$\Delta V_{TM_{o_1}} = -y \Delta i_{ph} r_D \left(1 - e^{-\left(\frac{t_f - t_o}{C r_D}\right)}\right)$$

$$\text{for } t_R \leq t_o \leq t_f \qquad (60A)$$

and

$$\Delta V_{TM_{o_1}} = -y\,\Delta i_{ph}\left[r_{11}\left(1 - e^{-\left(\frac{t_f - t_o}{C\,r_{11}}\right)}\right) + r_D\left(1 - e^{-\left(\frac{t_f - t_R}{C\,r_D}\right)}\right)\right]$$

$$\text{for } 0 < t_0 \leq t_R \tag{61A}$$

Equations (61A), (58A), (57A) and (54A) combine to define the complete time dependence of ΔV_{TM} once the light has been turned on.

VI.A Conclusions

The equivalent circuit developed in the introduction is useful in understanding the operation of the vidicon employing secondary emission. The parameters of the circuit may be determined in the dark if measurements are made at various temperatures as outlined in section II.A. Section III.A shows that the resolution is determined by the length of the beam in its direction of motion times the factor $\frac{C\,r_b}{t_R}\left(1 - e^{-t_R/C\,r_D}\right)$.

The response of the tube to a changing light level is shown to be limited by the time constant $\dfrac{t_f}{\left(t_R/C\,r_b + \dfrac{t_f - t_R}{C\,r_D}\right)}$

The parameter C_{TM}/C gives a coupling of the signal to information appearing on all the devices, even those not being read. It would therefore seem desirable to keep this parameter small.

If one were to compare the situation described here with that of a low beam velocity vidicon, a circuit similar to that described in Figure 3A could be employed where the mesh lead would be replaced by the cathode. In this case the parameter C_{TM}/C would be negligible compared to unity. The beam resistance r_b would be describable as

$$r_b \approx \frac{\overline{V_c}}{i_b} \tag{62A}$$

where $\overline{V_c}$ is the average energy of the electrons emitted from the cathode and i_b is the current. The generator $(\delta-1)\,i_b$ would not exist. The difficulty with the approach outlined

here for this problem is that i_b varies dramatically in this case between the beginning and end of the read time, so that r_b does not appear to be constant during the cycle. It is therefore better in the case of the low beam velocity tube to consider the beam current as the variable of interest during the cycle between successive reads [10], while it is better in the high beam velocity tube to consider target voltage as the variable of interest, as was done in this report.

APPENDIX B

POSITIVE AND NEGATIVE MODES OF HIGH BEAM VELOCITY OPERATION

In the discussion in Appendix A and in the main body of this report it was assumed that the target is being scanned by a monoenergetic beam of electrons of energy $e\ V_{TK}$, where V_{TK} is the target to cathode voltage. In actuality, this will not be the case, as a result of the generation of secondaries from the mesh and elsewhere. These electrons will land on the target with the main beam, and can influence the potential at which the target surface floats. Dresner [4] has recognized this type of problem, and points out the fact that in high beam velocity operation, the target surface can be charged either positively or negatively relative to the mesh without interfering with the details of its operation. Figure B1 [4] shows how mesh secondaries can influence the dependence of target current on V_{TK}. The presence of these secondaries will influence the ability to relate tube parameters to material properties, but as long as the target to mesh voltage is adjusted to keep the diode reverse biased, they will not affect imaging.

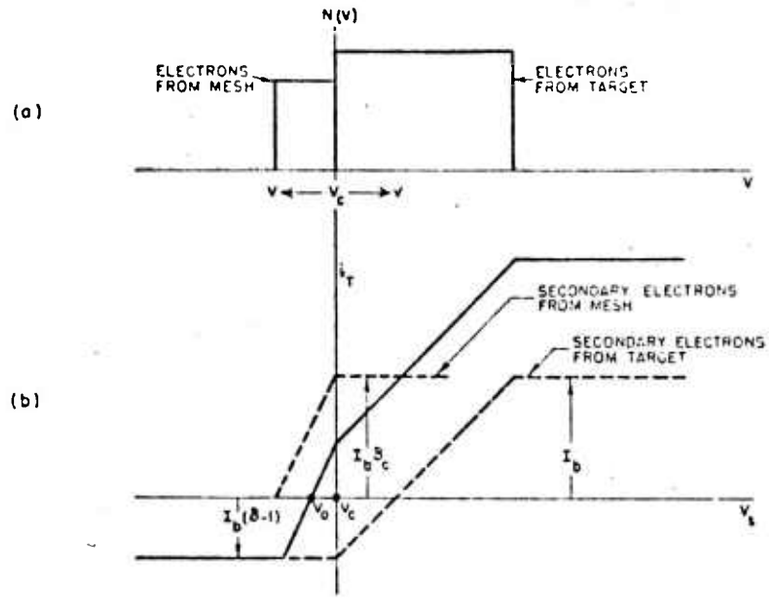

Figure B1

Effect of secondary electrons emitted from the mesh. When $V_o < V_c$, the beam conductance is controlled by the secondary electrons from the mesh.